Geological Society of America Special Papers Online First

Deccan volcanism, the Chicxulub impact, and the end-Cretaceous mass extinction: Coincidence? Cause and effect?

Gerta Keller

Geological Society of America Special Papers, published online June 10, 2014;
doi:10.1130/2014.2505(03)

The Geological Society of America
Special Paper 505
2014

Deccan volcanism, the Chicxulub impact, and the end-Cretaceous mass extinction: Coincidence? Cause and effect?

Gerta Keller*
Geosciences Department, Princeton University, Princeton, New Jersey 08544, USA

ABSTRACT

The recent discovery of the direct link between Deccan volcanism and the end-Cretaceous mass extinction also links volcanism to the late Maastrichtian rapid global warming, high environmental stress, and the delayed recovery in the early Danian. In comparison, three decades of research on the Chicxulub impact have failed to account for long-term climatic and environmental changes or prove a coincidence with the mass extinction. A review of Deccan volcanism and the best age estimate for the Chicxulub impact provides a new perspective on the causes for the end-Cretaceous mass extinction and supports an integrated Deccan-Chicxulub scenario. This scenario takes into consideration climate warming and cooling, sea-level changes, erosion, weathering, ocean acidification, high-stress environments with opportunistic species blooms, the mass extinction, and delayed postextinction recovery.

The crisis began in C29r (upper CF2 to lower CF1) with rapid global warming of 4 °C in the oceans and 8 °C on land, commonly attributed to Deccan phase 2 eruptions. The Chicxulub impact occurred during this warm event (about 100–150 k.y. before the mass extinction) based on the stratigraphically oldest impact spherule layer in NE Mexico, Texas, and Yucatan crater core Yaxcopoil-1. It likely exacerbated climate warming and may have intensified Deccan eruptions. The reworked spherule layers at the base of the sandstone complex in NE Mexico and Texas were deposited in the upper half of CF1, ~50–80 k.y. before the Cretaceous-Tertiary (K-T) boundary. This sandstone complex, commonly interpreted as impact tsunami deposits of K-T boundary age, was deposited during climate cooling, low sea level, and intensified currents, leading to erosion of nearshore areas (including Chicxulub impact spherules), transport, and redeposition via submarine channels into deeper waters. Renewed climate warming during the last ~50 k.y. of the Maastrichtian correlates with at least four rapid, massive volcanic eruptions known as the longest lava flows on Earth that ended with the mass extinction, probably due to runaway effects. The kill mechanism was likely ocean acidification resulting in the carbonate crisis commonly considered to be the primary cause for four of the five Phanerozoic mass extinctions.

*gkeller@princeton.edu

Keller, G., 2014, Deccan volcanism, the Chicxulub impact, and the end-Cretaceous mass extinction: Coincidence? Cause and effect?, *in* Keller, G., and Kerr, A.C., eds., Volcanism, Impacts, and Mass Extinctions: Causes and Effects: Geological Society of America Special Paper 505, doi:10.1130/2014.2505(03). For permission to copy, contact editing@geosociety.org.

INTRODUCTION

Two catastrophes coincided with the end-Cretaceous mass extinction: the Chicxulub impact on Yucatan and Deccan volcanism in India. For the past 30 yr, many scientists have claimed the Chicxulub impact to be the sole cause for the mass extinction (Schulte et al., 2010), though not without controversy (Archibald et al., 2010; Courtillot and Fluteau, 2010; Keller et al., 2010). Over the past 5 yr, research advances in Deccan volcanism have revealed its central role in this mass extinction, calling for reevaluation of Chicxulub and its presumed catastrophic effects. How each of these catastrophes contributed to or caused the mass extinction, either by itself or in combination, and whether they were coincident in time are still under investigation. Intense research of large igneous province volcanism identified four of the five big mass extinctions in Earth's history as coincident with large, rapid volcanic eruptions, revealing these catastrophes as much more deadly than previously assumed (Bond and Wignall, this volume; Courtillot and Fluteau, this volume). Only the K-T boundary mass extinction (also known as the Cretaceous-Paleogene boundary) coincides with both a large impact and one of the largest volcanic episodes in Earth's history. This study reviews recent advances in Deccan volcanism tying this catastrophe directly to the K-T boundary mass extinction, summarizes the best age estimate for the Chicxulub impact, and places these two catastrophes within their stratigraphic context relative to the mass extinction. This is a first step toward identifying the respective roles of impact and volcanism in the K-T boundary mass extinction.

Deccan volcanic eruptions once covered most of India, with an estimated 1.5 million km^2 and 1.2 million km^3 lava extruded, which even today, with about two thirds eroded or buried, still covers an area the size of France or Texas (Fig. 1). Flow after flow of volcanic eruptions piled up in horizontally layered sequences reaching several thousand meters, which today still form mountains up to 3500 m (Fig. 1; Bodas et al., 1988; Khadri et al., 1988; Chenet et al., 2007). Some massive eruptions reached over 1500 km across India and out to the Bay of Bengal via intracanyon transport (Baksi et al., 1994), forming the longest lava flows known on Earth (Self et al., 2008; Jay and Widdowson, 2008).

Until the early 1980s, Deccan eruptions were believed to have occurred over several million years (68–63 Ma, magnetic anomalies C31R to C28R), spanning most of the Maastrichtian to Early Danian. Subsequent studies determined that the bulk of eruptions clustered within less than 1 m.y. (C29r) spanning the K-T boundary, although the estimated uncertainty in the $^{40}Ar/^{39}Ar$ ages is 1%–2.5% (Courtillot et al., 1986, 1988; Vandamme et al., 1991; Hofmann et al., 2000; Sheth et al., 2001; Pande et al., 2004; Kuiper et al., 2008). More recently, detailed paleomagnetic studies combined with $^{40}K/^{40}Ar$ and $^{40}Ar/^{39}Ar$ dating of Deccan lava flows revealed three main volcanic phases of relatively short durations in the early late Maastrichtian, in C29R, and in the early Danian C29N (Chenet et al., 2007, 2008, 2009).

A potential cause-and-effect relationship between Deccan volcanism and the K-T boundary mass extinction was advocated by the early 1980s (McLean, 1978, 1985; Courtillot et al., 1986, 1988; Rice, 1990; Venkatesan et al., 1993; Jaiprakash et al., 1993; Raju et al., 1995). The evidence implicating Deccan volcanism in the K-T boundary mass extinction rested primarily on the sheer size of this volcanic province, the C29R age, and the association of three other mass extinctions with major volcanic provinces

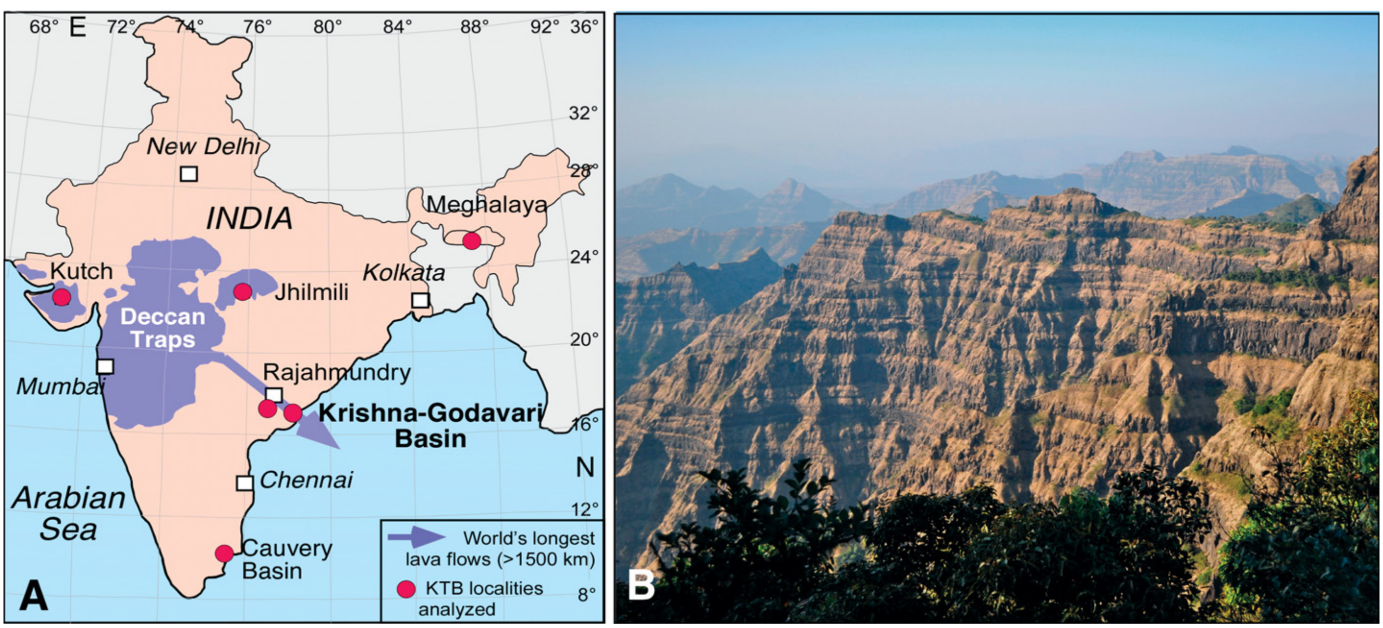

Figure 1. (A) Map of India with current distribution of the Deccan Traps, including the longest lava flows to the Krishna-Godavari Basin, and localities analyzed. KTB—K-T boundary. (B) Photo of Deccan Traps in the mountains of Mahabaleshwar.

(Permian-Triassic, Triassic-Jurassic, and end-Devonian; Wignall, 2001; Courtillot and Renne, 2003; Bond and Wignall, this volume). This suggested that large igneous provinces could have been the general cause of mass extinctions.

Acceptance of Deccan volcanism as a catastrophe that could have led to the extinction of the dinosaurs and many other groups has lagged for three main reasons: (1) the popularity of the Chicxulub impact as the cause for the mass extinction, (2) the belief that Deccan volcanism occurred over at least 1 m.y., leaving sufficient time for recovery between eruptions, and (3) the absence of data that directly linked the mass extinction with Deccan volcanism in India. Research discoveries over the past several years have largely laid these concerns to rest. Critical factors in this development have been the paleomagnetic and $^{40}K/^{40}Ar$ and $^{40}Ar/^{39}Ar$ dating of Deccan lava flows demonstrating three main phases of eruptions (Chenet et al., 2007, 2008, 2009; Jay and Widdowson, 2008; Jay et al., 2009), and the discovery that the main phase 2 eruptions are directly linked to the end-Cretaceous mass extinction (Keller et al., 2008, 2009a, 2009b, 2009c, 2011a, 2012).

This paper reviews and summarizes the evidence accumulated over the past few years that links Deccan volcanism to the K-T boundary mass extinction as recorded in planktic foraminiferal populations in India. These unicellular calcareous shelled organisms suffered the most severe mass extinctions among marine organisms worldwide. In addition, the link between Deccan volcanism and the Chicxulub impact is explored, and the age of the Chicxulub impact is estimated based on the stratigraphically oldest impact ejecta (e.g., impact spherules, impact breccia). Key points addressed include: (1) the direct link between Deccan volcanism and the K-T boundary mass extinction in India, (2) the nature and timing of the mass extinction associated with volcanism, (3) the geochemical markers of climate and environmental changes related to volcanism, (4) the global biotic effects of Deccan volcanism as recognized in species dwarfing and blooms of the disaster opportunist *Guembelitria cretacea*, (5) the age of the Chicxulub impact based on the stratigraphic position of the oldest (primary) impact ejecta layer, (6) the coincidence between Deccan volcanism and the Chicxulub impact relative to the K-T boundary and mass extinction, and (7) the climate changes associated with phase 2 Deccan volcanism and the Chicxulub impact.

STRATIGRAPHY OF DECCAN VOLCANISM AND CHICXULUB IMPACT

Radiometric Dating

Age determinations of the Deccan Traps are based on paleomagnetism and $^{40}K/^{40}Ar$ and $^{40}Ar/^{39}Ar$ dating in west-central India, where basalts form nearly horizontally deposited beds (dip ~1°) for the entire 3500-m-thick lava pile that extend from 16°N to 25°N and from 70°E to 79°E (Fig. 1; Chenet et al., 2007). It is now generally accepted that Deccan volcanism occurred mainly in three major phases. The initial Deccan eruption phase 1 is dated early late Maastrichtian (ca. 67.4 Ma, base C30N) and accounts for ~6% of the 3500-m-thick total Deccan lava pile (Fig. 2). For the next ~1.5 m.y. (C30N into lower C29R), volcanic activity seems to have been absent or inconsequential. The main Deccan phase 2 eruptions occurred over a relatively short time interval in C29R and account for ~80% of the total lava pile (Chenet et al., 2007, 2008, 2009). Biostratigraphic data demonstrate that this volcanic phase ended with the mass extinction, as reviewed herein (Keller et al., 2008, 2011a, 2012). Over the next 200–300 k.y. of the early Paleocene (Danian, C29R above the K-T boundary), volcanic activity was inconsequential or absent. The last Deccan eruption, phase 3, began near the base of C29N and accounts for ~14% of the total Deccan lava pile (Fig. 2). Associated with phase 2 and phase 3 are the largest and longest lava megaflows known on Earth, spanning 1500 km across India and out into the Bay of Bengal (Fig. 1; Self et al., 2008; Keller et al., 2008, 2011a, 2012).

Although the three main phases of Deccan volcanism are well documented, the dating techniques based on $^{40}K/^{40}Ar$ and $^{40}Ar/^{39}Ar$ are imprecise due to uncertainties in the standards used and radioactive decay rates, which reduce absolute age accuracy up to 2.5% (Kuiper et al., 2008). Nevertheless, a recent study by Renne et al. (2013) claimed that the Chicxulub and the K-T boundary mass extinction were synchronous within 32,000 yr based on $^{40}Ar/^{39}Ar$ ages from bentonite layers from Hell Creek, Montana, and 16 impact spherules from Haiti. To date, only U-Pb isotope dilution–thermal ionization mass spectrometry (ID-TIMS) zircon

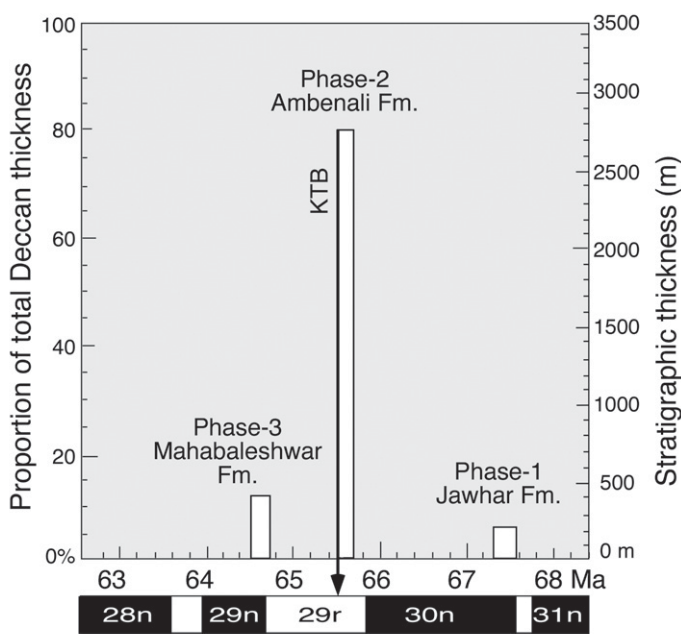

Figure 2. Relative thickness of Deccan lava flows in each of the three phases of volcanic eruptions calculated as percent of total Deccan Trap thickness. Ages are based on paleomagnetic time scale (modified from Chenet et al., 2007, 2008).

geochronology is capable of achieving better than ±60–100 k.y. accuracy based on single-zircon crystal analyses with analytical precision of ±0.02%. Dating of the Deccan Traps material based on U-Pb ages has been unsuccessful to date due to the rarity or absence of zircon crystals in the lava flows, and U-Pb age determinations for the K-T boundary are lacking. Thus, the establishment of better age control for Deccan volcanism and the Chicxulub impact based on radiometric dating has remained elusive.

Relative Dating—Biostratigraphy

Even the best absolute dating methods may not distinguish the order of closely spaced events within the narrow time interval of the K-T boundary mass extinction, Chicxulub impact, and Deccan volcanism, all of which may have occurred within an interval of less than 160 k.y. (planktic foraminiferal zone CF1). Identifying the relative order of such closely spaced events remains the domain of relative dating based on lithostratigraphy (relative order of sediment layers from old to young), biostratigraphy, and stable isotope stratigraphy (Keller, 2008).

Biostratigraphy focuses on correlating rock strata based on shared fossil species or species assemblages without regard to lithology and is arguably the most reliable relative age dating technique in stratigraphy. It makes use of the fossil record and its unique evolutionary events, such as species originations and extinctions, unique population turnovers, and individual species blooms, and ties these to the paleomagnetic and radiometric records. Relative age dating of marine sediments globally, and specifically sequences with Chicxulub impact ejecta and Deccan volcanism, is based on the high-resolution planktic foraminiferal zonal scheme developed by Keller et al. (1995, 2002a) for the Danian and by Li and Keller (1998a, 1998b) for the Maastrichtian (Fig. 3). This zonation was developed based on planktic foraminifera from the El Kef stratotype and Elles sections in Tunisia and sections from the eastern Tethys, Madagascar, Spain, and South Atlantic.

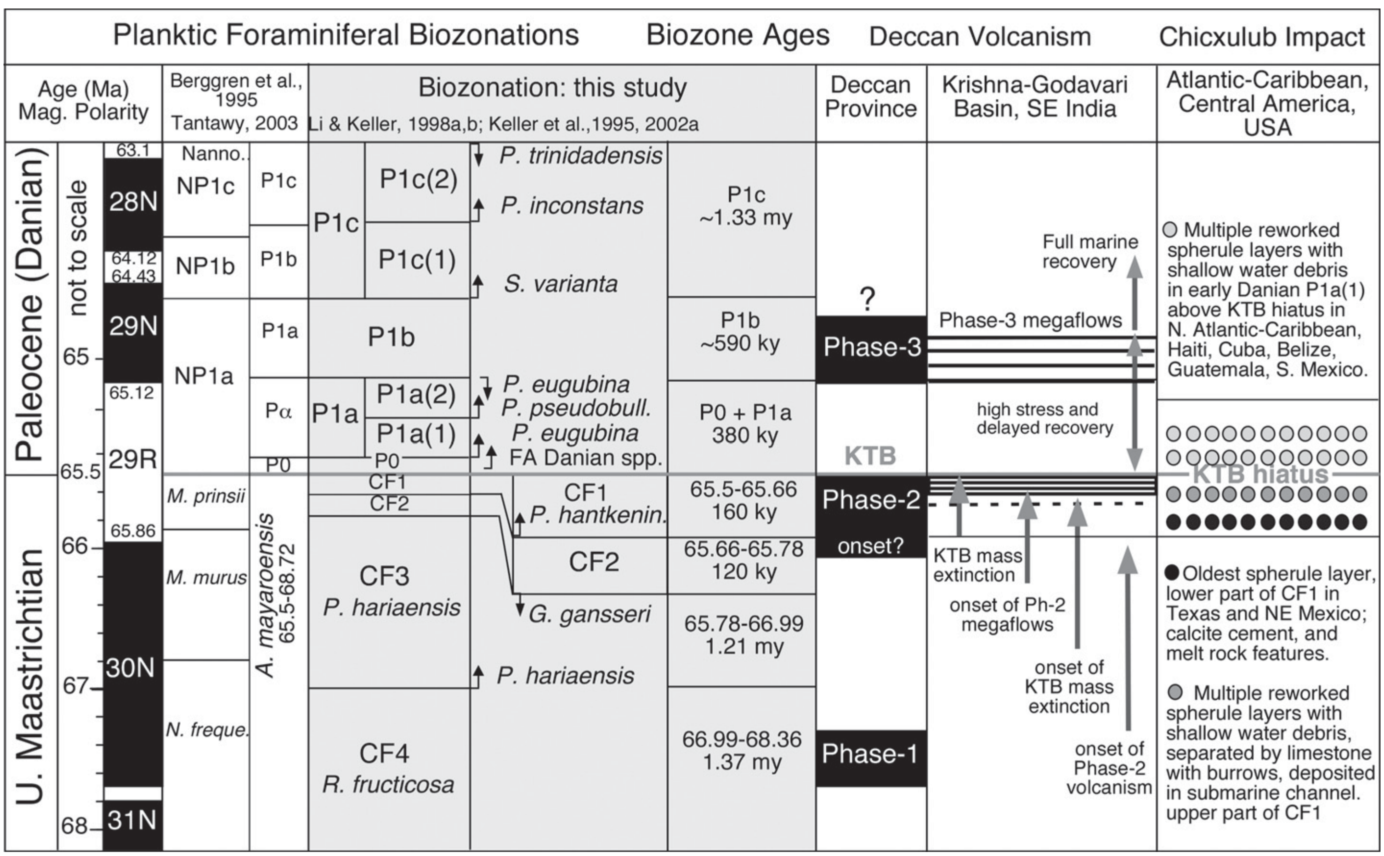

Figure 3. Late Maastrichtian and early Paleocene (Danian) planktic foraminiferal zonal schemes and ages of biozones calculated based on the time scale of Gradstein et al. (2004) with the K-T boundary (KTB) at 65.5 Ma. The stratigraphic position of Deccan megaflows and the onset of the K-T boundary mass extinction in the Krishna-Godavari Basin are based on this study (modified from Keller et al., 2011a). Genus abbreviations: *M. prinsii—Micula prinsii*; *M. murus—Micula murus*; *N. freque.—Nephrolithus frequens*; *A. mayaroensis—Abathomphalus mayaroensis*; *G. gansseri—Gansserina gansseri*; *P. hariaensis—Pseudoguembelina hariaensis*; *P. hantkenin.—Plummerita hantkeninoides*; *P. eugubina—Parvularugoglobigerina eugubina*; *P. pseudobull.—Parasubbotina pseudobulloides*; *P. inconstans—Praemurica inconstans*; *P. trinidadensis—Praemurica trinidadensis*; *R. fructicosa—Racemiguembelina fructicosa*; *S. varianta—Subbotina varianta*.

K-T Boundary Identifying Criteria

From the stratigraphic and paleontologic point of view, the most critical event in Deccan history is identifying the position of the mass extinction in the Deccan lava pile and determining whether there is a cause-and-effect relationship. Similarly, determining the age of the Chicxulub impact relative to the mass extinction is the most important stratigraphic problem of the K-T boundary event. To date, the Chicxulub impact is *assumed* to have caused the mass extinction, and this *belief*, rather than stratigraphic data, has led to a redefinition of the K-T boundary based on Chicxulub impact ejecta (discussed herein).

The K-T boundary is one of the most easily identified boundary events in geological history (Keller, 2011). A set of five K-T boundary–identifying criteria, originally proposed by the International Commission on Stratigraphy (ICS) and the International Union of Geological Sciences (IUGS) working group during 1980-1990s, has proven globally applicable and independently verifiable: (1) the mass extinction of Cretaceous planktic foraminifera, (2) evolution of the first Danian species, (3) K-T boundary clay and red layer, (4) Ir anomaly, and (5) $\delta^{13}C$ shift (Cowie et al., 1989; Keller et al., 1995; Remane et al., 1999).

Planktic foraminifera are the only marine microfossil group that suffered near-total and relatively abrupt mass extinction across the K-T boundary, leaving just one long-term survivor—*Guembelitria cretacea*. The evolution of new species from this survivor followed almost immediately. These unique bioevents, the mass extinction and evolution of new planktic foraminifera, have remained the most reliable K-T boundary–defining criteria worldwide. All other K-T boundary markers, such as the $\delta^{13}C$ shift, clay layer, red layer, and Ir anomaly, including impact glass spherules, are useful supporting evidence but not unique signals in the geological record due to reworking and redeposition. Therefore, impact signals cannot define the K-T boundary in the absence of unique biomarkers (Keller, 2011). In the Deccan Traps, the K-T boundary has now been identified in several localities in central and southeastern India based on the standard defining criteria (mass extinction, evolution of first Danian species; Keller et al., 2011a, 2012) and in one locality (Meghalaya) based on the defining criteria as well as all supporting criteria (Gertsch et al., 2011a).

The same defining and supporting criteria have been successfully applied to hundreds of K-T boundary localities worldwide, including over 100 sequences in the North Atlantic, Caribbean, Central America, and the United States, many of which contain Chicxulub impact ejecta, particularly melt-rock glass spherules. In these sequences, the stratigraphic position of the impact ejecta relative to the K-T boundary provides critical information on the timing of this impact. However, the presence of multiple impact glass spherule layers in many sequences and their stratigraphic position below, at, and above the K-T boundary indicate that impact ejecta can be easily eroded, transported, and redeposited after primary deposition (Fig. 3; Keller, 2008). Stratigraphy's challenge is to decode these multiple depositional events and identify the primary (oldest) impact ejecta layer that pinpoints the time of the Chicxulub impact.

Impact signals are not of significant concern in India. No impact glass spherules have been found, and the only major Ir anomaly is known from the Meghalaya section (Bhandari et al., 1993, 1994; Gertsch et al., 2011a). A minor Ir anomaly reported from the Anjar section in Kutch and originally identified as K-T boundary age (Bhandari et al., 1996; Courtillot et al., 2000) is of volcanic origin and late Maastrichtian age (e.g., Bajpai and Prasad, 2000; Sant et al., 2003). Chatterjee et al. (2006) suggested a crater (Shiva) off Mumbai and impact ejecta at various localities in India, though none has been confirmed.

Chicxulub Defined as K-T Boundary Age

In recent years, impact markers, such as Ir anomalies and impact glass spherules, have frequently been used as the sole markers for the K-T boundary based on the *belief* that the Chicxulub impact caused the mass extinction (e.g., Olsson et al., 1997; Norris et al., 1999, 2000; Arenillas et al., 2006; Molina et al., 2006; MacLeod et al., 2007; Schulte et al., 2010). This practice resulted in redefinition of the K-T boundary based solely on impact markers, particularly impact spherules and Ir anomaly (Molina et al., 2006), which resulted in circular reasoning and delayed recognition of the true age of the Chicxulub impact (Keller, 2008, 2011; Keller et al., 2013). Impact spherules are frequently reworked in late Maastrichtian and early Danian sediments; therefore, designating a layer close to the K-T boundary as the age of Chicxulub is arbitrary.

Iridium anomalies are easily remobilized and reconcentrated at redox layers (e.g., Colodner et al., 1992; Miller et al., 2010; Gertsch et al., 2011a, 2011b). Therefore, small (<1–1.5 ppb) Ir anomalies are unreliable impact markers. To date, out of 345 K-T boundary sections worldwide, just 85 have Ir enrichments, and only five localities have large Ir anomalies: Denmark, Tunisia (El Kef and Elles), Meghalaya, India, and New Zealand (Schmitz et al., 1992; Bhandari et al., 1994; Gertsch et al., 2011a; Premovic et al., 2012). These large Ir anomalies are concentrated at redox boundaries (red clay layers) and reflect significant Ir influx from nearby marine and continental sites (Premovic et al., 2012). No Ir anomaly has ever been detected in Chicxulub impact ejecta. The small (<1 ppb) Ir enrichments commonly reported (e.g., Norris et al., 1999, 2000; Arenillas et al., 2006; Schulte et al., 2010) are above a K-T boundary hiatus and above reworked impact spherules in early Danian sediments (Keller et al., 2013).

DECCAN VOLCANISM LINKED TO MASS EXTINCTION

Although numerous studies over the past 30 yr have advocated Deccan volcanism as the potential cause for the K-T boundary mass extinction (e.g., McLean, 1985; Courtillot et al., 1986, 1988; Jaiprakesh et al., 1993), no direct link could be established in these continental flood basalts. Ideally, a direct link consists of basalt flows separated by marine sediments with microfossils recording the mass extinction. Only in extreme outlying areas of the Deccan volcanic province, such as the Krishna-Godavari (K-G) Basin of southeastern India, are marine sediments present together with Deccan Trap basalts (Fig. 4). For example, in the Rajahmundry area, numerous quarries expose Deccan Traps once deposited along the paleoshoreline (Keller et al., 2008). Further seaward in the Krishna-Godavari Basin, the Deccan Traps are buried 2500–3500 m below the surface. In central India (Jhilmili, Chhindwara), an intertrappean bed representing a marine incursion was discovered (Keller et al., 2009a, 2009b). The best K-T boundary sequence in India is known from Meghalaya, NE India, ~800 km from the Deccan volcanic province. This section is critically important because it records the stress conditions related to Deccan volcanism and ties these with the global record (Garg et al., 2006; Gertsch et al., 2011a).

Um Sohryngkew, Meghalaya

The Um Sohryngkew section of Meghalaya is located along the river that bears its name and runs along the border with Bangladesh (Fig. 1). This section has one of the most complete K-T boundary records worldwide, containing all K-T boundary defining and supporting criteria, including the mass extinction, evolution of first Danian species, $\delta^{13}C$ shift, the boundary clay, and a thin red layer with an Ir anomaly of 12 ppb (Fig. 5; Gertsch et al., 2011a). This large Ir anomaly and other platinum group element anomalies are attributed to an extraterrestrial impact, condensed sedimentation, redox fluctuations, and volcanism (Pandey, 1990; Bhandari et al., 1993, 1994; Garg et al., 2006; Gertsch et al., 2011a).

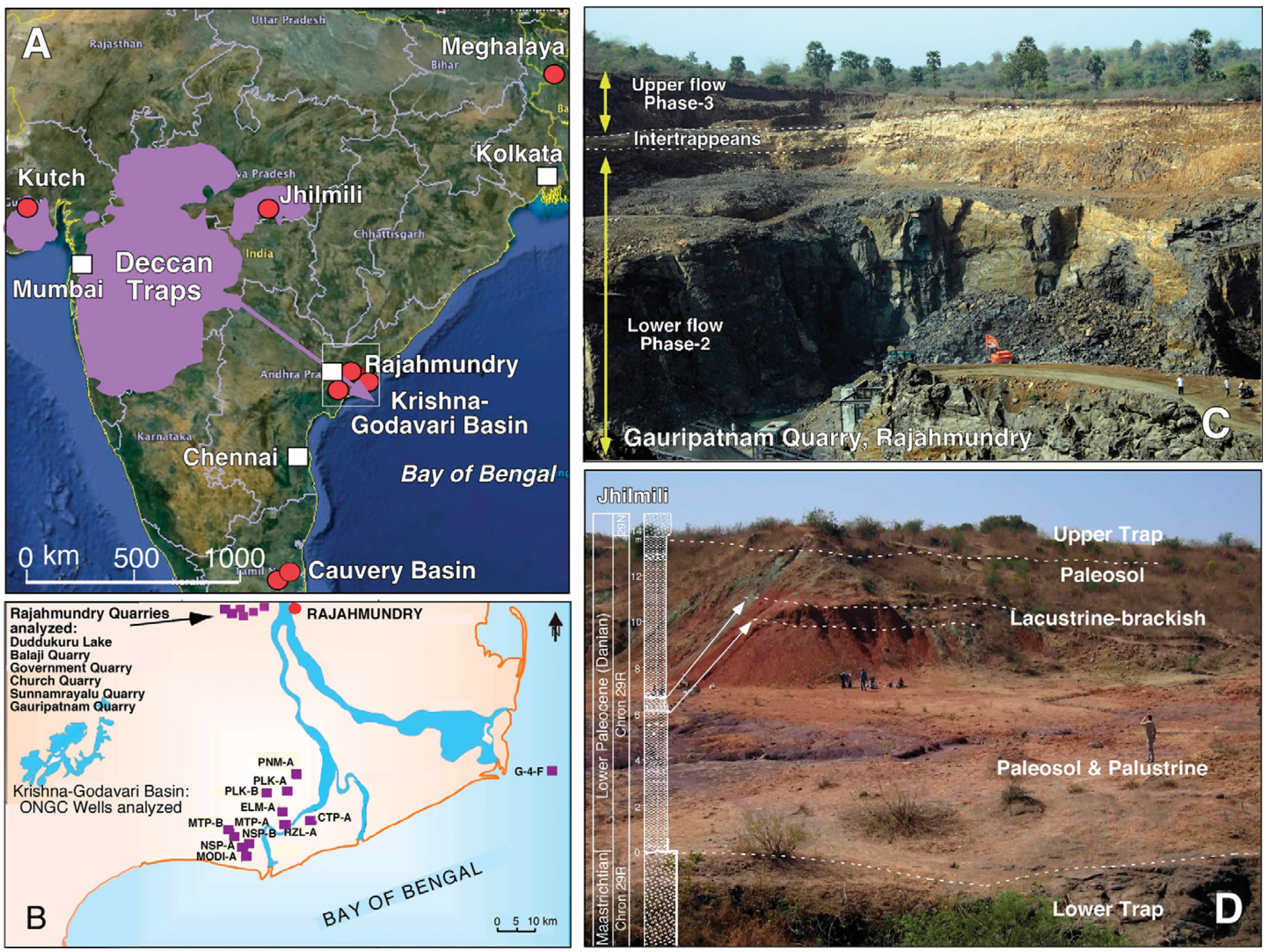

Figure 4. Location map and photos of outcrops analyzed at Jhilmili and the Rajahmundry area, and locations of deep wells analyzed in the Krishna-Godavari Basin and outcrop in Jhilmili, central India. (A) Location map; (B) outcrop and bore well locations in the Krishna-Godavari Basin; (C) Gauripatnam Quarry with intertrappean sediments of earliest Danian age in Rajahmundry; (D) outcrop in Jhilmili, central India, with intertrappean sediments of earliest Danian zone P1a age.

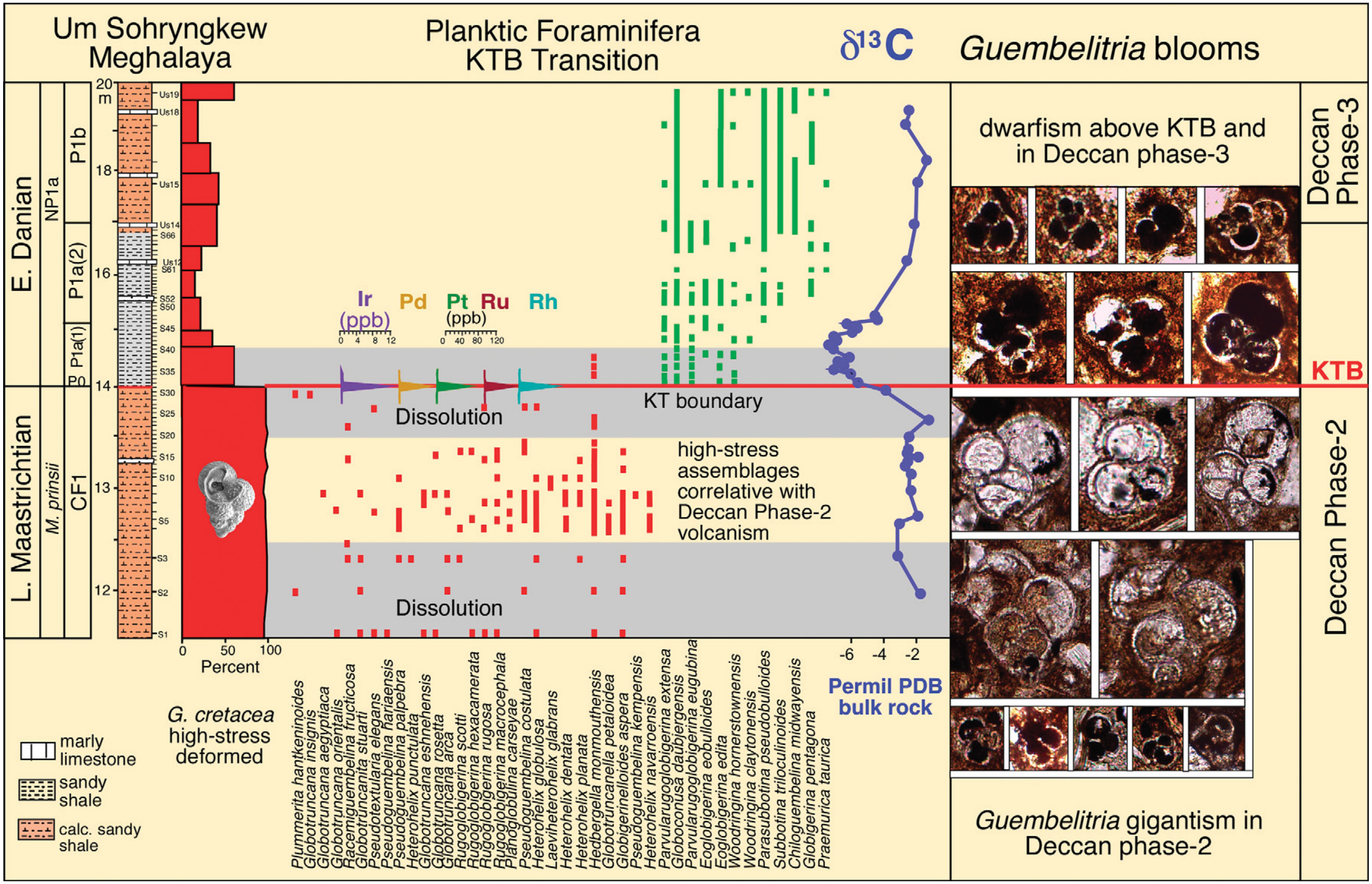

Figure 5. The K-T boundary (KTB) transition at Um Sohryngkew, Meghalaya, one of the most complete boundary sequences worldwide, shows superstress conditions in planktic foraminifera of the latest Maastrichtian (zones CF1–2, *Micula prinsii*) as evident in *Guembelitria* blooms, dwarfing and gigantism, sporadic occurrences of other species, and effects of ocean acidification. Size changes in *Guembelitria cretacea* in zone CF1 (*M. prinsii*) correlative with volcanic phase 2 (magnification is the same for all specimens): small dwarf size (bottom row) near the base of the CF1 interval; gigantism (rows 2 and 3) through most of CF1; normal size of species (row 4) above the K-T boundary mass extinction; return to small dwarfed morphotypes in zone P1b (row 5) correlative with Deccan phase 3. PDB—Peedee belemnite. Figure is modified from Gertsch et al. (2011a).

The latest Maastrichtian zone CF1 below the K-T boundary has low planktic foraminiferal diversity (total 28 species), but less than half are generally present in any one sample due to rare and sporadic occurrences and variable carbonate dissolution (Fig. 5). Species assemblages are dominated by *Guembelitria cretacea*, which account for more than 95% of the total planktic foraminiferal population. The low species diversity, rare and sporadic occurrences, and dominance of *Guembelitria cretacea* are characteristics of high-stress environments, whereas the carbonate dissolution suggests lower pH due to ocean acidification.

Above the K-T boundary, the $\delta^{13}C$ shift and earliest Danian species indicate zone P1a (subzones P1a[1] and P1a[2]; Fig. 3). In P1a(1), *Guembelitria* specimens decrease in abundance correlative with minimum $\delta^{13}C$ values and increase again in zone P1b after the extinction of *Parvularugoglobigerina eugubina*. This pattern and the sequence of species evolution in the early Danian follow global patterns (Punekar et al., this volume).

The most unusual aspects in the Um Sohryngkew K-T boundary transition are the extreme abundance (>95%) and very large size of *Guembelitria cretacea* in zone CF1. This species is normally a very small triserial morphotype, frequently common to abundant in the 36–63 µm size fraction and almost always <100 µm in size. However, in this section, very large morphotypes frequently exceeding 150 µm dominate (~85%). A size comparison is illustrated in Figure 5 based on the same magnification for all specimens. The bottom row shows normal small species of zone CF1, compared with rows 2 and 3 illustrating the predominantly large morphotyes of the assemblage. Above the K-T boundary, the normal small morphotypes dominate with few large ones. A survey of zone CF1 *Guembelitria cretacea* populations in the eastern Tethys reveals similar dominance, but large morphotypes are rare (Punekar et al., this volume).

Guembelitria blooms are indicative of high-stress environments and are most commonly recorded from the aftermath of the K-T boundary mass extinction (Pardo and Keller, 2008; Keller and Abramovich, 2009). Their dominance in zone CF1 below the K-T boundary records extreme high-stress conditions correlative with the main phase 2 of Deccan volcanism, whereas their high abundance in the early Danian zone P1b is correlative with phase 3 (Figs. 2 and 5; Keller et al., 2012). In Meghalaya, the *Guembelitria* dominance in the latest Maastrichtian is associated with geochemical and mineralogical data that reveal humid climate conditions and periodic acid rains (carbonate dissolution) related to pulsed Deccan eruptions, and strong continental weathering and runoff resulting in mesotrophic waters (Gertsch et al., 2011a). These superstress conditions likely led to the demise of nearly all planktic foraminifera and blooms of the disaster opportunist *Guembelitria cretacea*. The Meghalaya section thus provides strong evidence for a close correlation between the global mass extinction record and Deccan volcanism, but a direct link within the Deccan Traps remained elusive until the discoveries in central and southeastern India.

Jhilmili, Central India

A surprising discovery of early Danian zone P1a planktic foraminifera was made through routine ostracod analysis of a 14-m-thick predominantly terrestrial intertrappean bed at Jhilmili, Chhindwara District, Madhya Pradesh (Figs. 4D and 6; Keller et al., 2009a, 2009b). These intertrappean sediments were believed to be terrestrial in origin and late Maastrichtian in age. The presence of rare early Danian freshwater and brackish marine ostracods (Khosla et al., 2009; Sharma and Khosla, 2009; Bajpai et al., 2013) and zone P1a planktic foraminifera in a narrow (0.60 m) interval between lower (phase 2) and upper (phase 3) basalt flows confirmed the link between the main phase 2 Deccan volcanism and the mass extinction. However, this discovery also revealed the presence of a major seaway depositing marine plankton in central India. The seaway likely followed the Narmada-Tapti rift, extending from the west 800 km across India (Keller et al., 2009a). Such a seaway already existed during the late Cenomanian marine transgression (Badve and Ghare, 1977) and was hypothesized to have existed during the late Maastrichtian to explain the high concentration of dinosaur nesting sites and other remains along the Narmada-Tapti rift zone (Sahni, 1983; Keller et al., 2009c).

Rajahmundry Quarries, SE India (Krishna-Godavari Basin)

The world's longest lava megaflows are known to have reached the Krishna-Godavari Basin during the latest Maastrichtian and again in the early Danian, ~300 k.y. after the mass extinction (Self et al., 2008; Keller et al., 2008). In the Rajahmundry area, Deccan basalts are quarried, exposing one thick intertrappean bed (Figs. 4C and 4D). The basalt megaflows below and above the intertrappean bed are generally known as lower and upper traps, which correspond to phase 2 and phase 3 of Deccan volcanism, respectively (Fig. 2). Paleomagnetic data identify the lower traps and the intertrappean sediments as C29R and the upper traps as C29N (Subbarao and Pathak, 1993). Age determinations to date are based on $^{40}K/^{40}Ar$ and $^{40}Ar/^{39}Ar$ dates of plagioclase separates (Knight et al., 2003, 2005; Chenet et al., 2007, 2008), which have large errors (1%–2.5%) that permit no determination of the K-T boundary position.

Early studies of intertrappean sediments in Rajahmundry quarries yielded a Danian age based on ostracods (Bhandari, 1995; Khosla and Nagori, 2002). A study of planktic foraminifera in four Rajahmundry basalt quarries recovered an earliest Danian zone P1a assemblage near the base of the intertrappean bed (Figs. 7 and 8), revealing the first direct link between the K-T boundary mass extinction and Deccan volcanism (Keller et al., 2008; Malarkodi et al., 2010; subsequently confirmed at Jhilmili, see previous section "Jhilmili, Central India"; Fig. 6). Intertrappean sediments in all quarries examined show similar biostratigraphy and depositional environments, although the thicknesses of individual units are variable, and some may not be present in

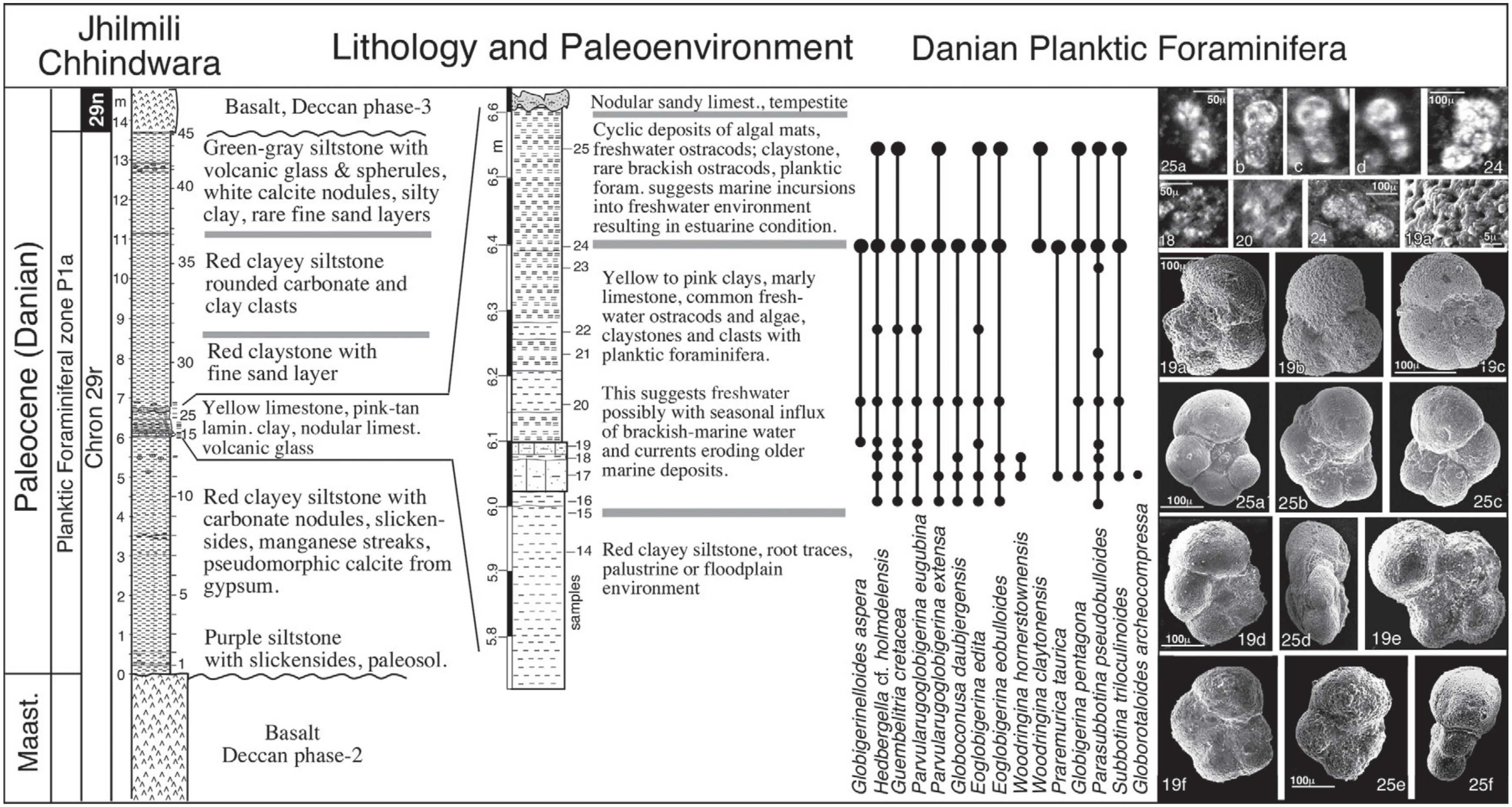

Figure 6. Early Danian intertrappean bed at Jhilmili, Chhindwara District, Madhya Pradesh, shows temporary marine incursion, with earliest Danian zone P1a planktic foraminifera indicating a seaway existed into central India. Larger circles mark samples with common foraminifera. Small planktic foraminiferal species are illustrated from thin section micrographs. Scale bar is the same for each row, unless otherwise indicated; numbers refer to samples. Top row images: 24, 25a–d—*Parasubbotina pseudobulloides*; 18, 20—*Parvularugoglobigerina eugubina*; 19a—scanning electron microscope images of cancellate spinose wall texture with calcite overgrowth of chambers in: 19a, 19b, 19c—*Subbotina triloculinoides*; 25a–c, 19d—*Parasubbotina pseudobulloides*; 19e, 25d—*Hedbergella* cf. *holmdelensis*; 19f—*Globigerina pentagona*; 25e—*Subbotina triloculinoides*; 25f—*Globigerinelloides aspera*. Figure is modified from Keller et al. (2009b).

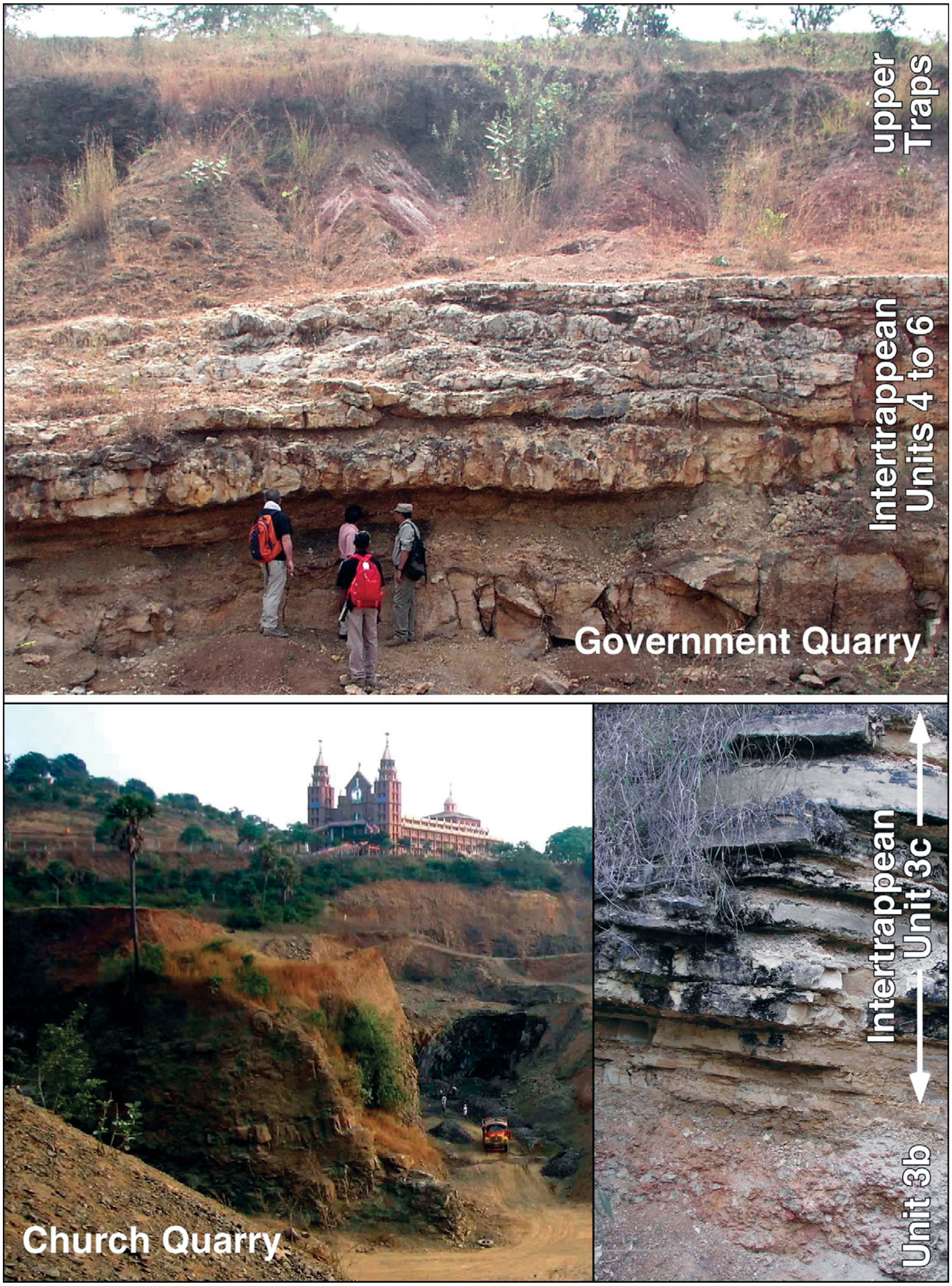

Figure 7. Photos of two Deccan basalt quarries (Government and Church Quarries) in the Rajahmundry area showing thick intertrappean beds with blowup of 1-m-thick unit 3b at the Church Quarry with earliest Danian zone P1a planktic foraminifera directly overlying the main phase 2 of Deccan volcanism.

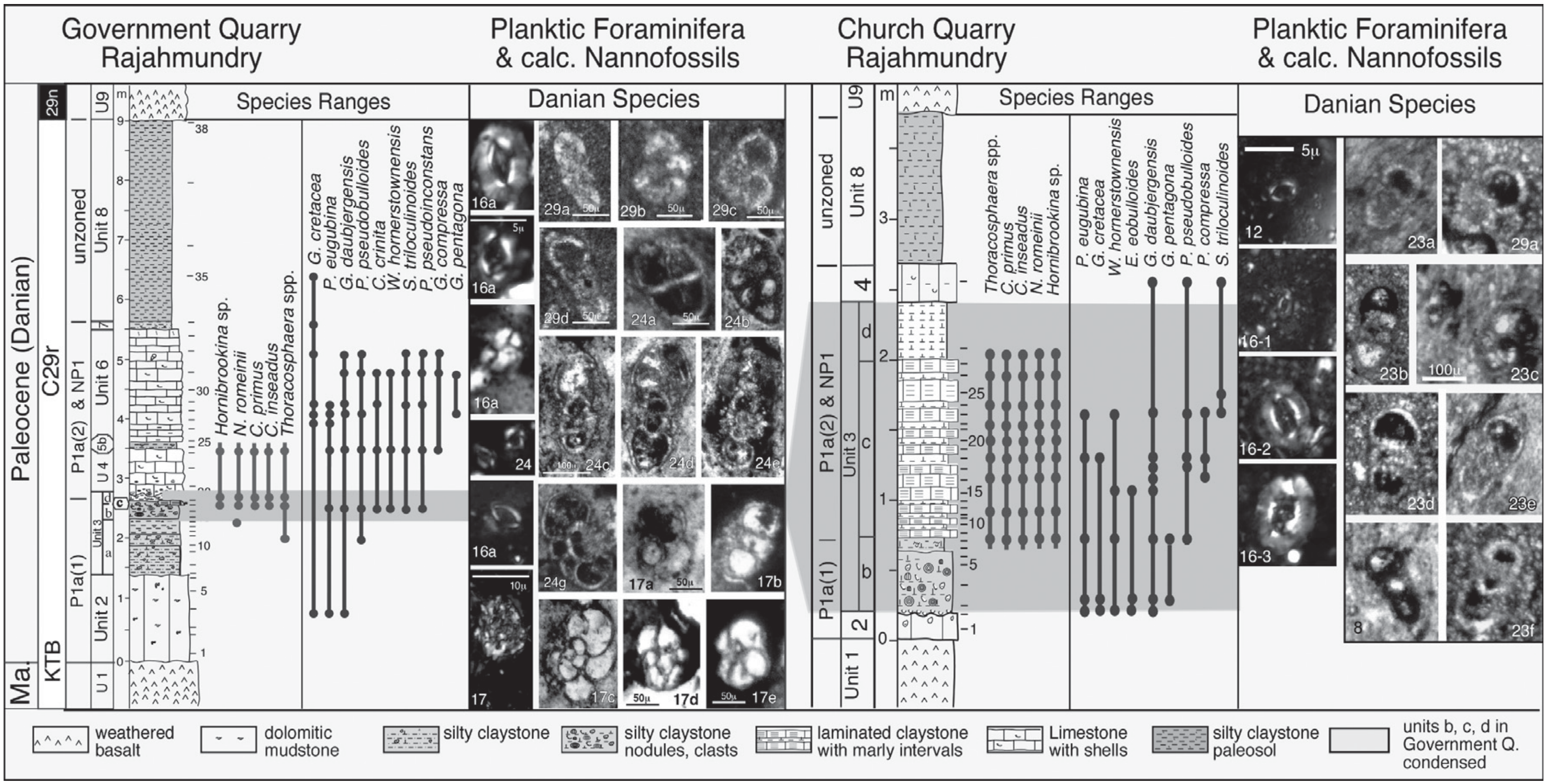

Figure 8. Government and Church Quarry biostratigraphy and species ranges of planktic foraminifera and calcareous nannofossils illustrated by photomicrographs. KTB—K-T boundary. Government Quarry (numbers keyed to samples in lithologic column): Calcareous nannofossils (scale bar = 5 µm for the first five species): 16a-1—*Cruciplacolithus* cf. *C. inseadus*; 16a-2—*Cruciplacolithus primus*; 16a-3—*Octolithus multiplus*; 24—*Neobiscutum romeinii*; 16a-4—*Hornibrookina* sp.; 17—*Thoracosphaera* spp. fragment. Planktic foraminifera: 29a, b, 17d, e—*Parvularugoglobigerina eugubina*; 29c, 24a, 17a—*Globoconusa daubjergensis*; 24b—*Chiloguembelina* sp.; 29d—*Globanomalina compressa*; 24c, d, g, 17c—*Parasubbotina pseudobulloides*; 24e—*Subbotina triloculinoides*. Church Quarry species (numbers keyed to samples in lithologic column): Calcareous nannofossils (scale bar = 5 µm): 12—*Neobiscutum romeinii*; 16-1—*Cruciplacolithus*? cf. *C. primus* (small morphotype); 16-2—*Cruciplacolithus* cf. *C. inseadus*; 16-3—*C. primus*. Planktic foraminifera (scale bar = 100 µm): 8—*Parvularugoglobigerina eugubina*?; 23a, 29a—*Globoconusa daubjergensis*; 23b, c, e, f—*Parasubbotina pseudobulloides*; 23d—*Subbotina triloculinoides*. Figure is modified from Keller et al. (2008).

all outcrops, as shown for the Government and Church Quarries (Figs. 7 and 8).

Sediments above the lower trap (phase 2) basalt begin with dolomitic mudstone with clasts containing small, earliest Danian planktic foraminifera indicative of zone P0 or base of zone P1a (Figs. 3 and 8). Above this interval, sediments vary from silty claystone with rare shells and foraminifera to limestones with common shells, calcareous nannofossils (early Danian NP1), and foraminifera indicative of zone P1a (Fig. 8). The lower and upper parts (units 3a and 6) of this interval are well represented in the Government Quarry, whereas the middle part (units 3b, 3c, and 3d) is well developed in the Church Quarry. The upper intertrappean sediments consist of paleosol directly underlying the upper trap phase 3 basalt.

Sediments and planktic foraminifera thus indicate a sea-level transgression at the base of the Danian, followed by fluctuating estuarine to inner neritic environments. The return to terrestrial deposition occurred prior to phase 3 eruptions (Fig. 8; Keller et al., 2008). Biostratigraphic data from the Rajahmundry quarries represent the first direct evidence of the earliest Danian evolution in planktic foraminifera immediately above the lower trap phase 2 megaflows. This indicates that the mass extinction must have coincided with the longest megaflows at the end of phase 2 Deccan volcanism, but this hypothesis cannot be tested in the Rajahmundry area because the prevailing sandy estuarine environment prior to Deccan phase 2 megaflows lacks planktic foraminifera. The best chance for a marine record is in deep wells of the Krishna-Godavari Basin seaward from Rajahmundry.

Deep Wells of the Krishna-Godavari Basin

Earlier studies of the Krishna-Godavari Basin, ~75 km east of Rajahmundry toward the Bay of Bengal, reported marine microfossils spanning the K-T boundary in deep wells (2500–3500 m below surface) drilled by India's Oil and Natural Gas Corporation (ONGC; Figs. 4A and 4B). Although the precise position of the K-T boundary event could not be determined by these studies, the information presented was promising. In most wells, up to eight lava flows were observed correlative with Deccan phase 3 and phase 2 Deccan Traps of Rajahmundry (Fig. 9). Most basalt layers are separated by relatively thin beds of sediments, and one thick sediment layer separates lower and upper basalt flows with reported Danian planktic foraminifera (Govindan, 1981; Jaiprakash et al., 1993; Raju et al., 1994, 1995), dinoflagellates (Mehrotra and Sargeant, 1987), calcareous nannoplankton (Saxena and Misra, 1994), and palynomorphs (Prasad and Pundeer, 2002).

In collaboration with ONGC scientists, we set out to study 12 wells in the Krishna-Godavari Basin (Fig. 4B) to test two hypotheses: (1) Deccan volcanism may have been the main cause of the K-T boundary mass extinction, possibly as a result of the giant phase 2 megaflow eruptions and their environmental consequences (the Meghalaya section provides support for this hypothesis although no direct link to the Deccan Traps; Fig. 5; see "Um Sohryngkew, Meghalaya" section); and (2) the long delayed post–K-T boundary recovery was the result of Deccan phase 3 volcanism in C29N. Results were published in Keller et al. (2011a, 2012), and key results are summarized next.

Lithology, Depositional Setting, and Megaflows

In the ONGC deep wells from the Krishna-Godavari Basin, sediment deposition occurred in a middle shelf environment that deepened eastward (~100–150 m; Jaiprakash et al., 1993; Raju et al., 1994; Keller et al., 2011a). The K-T boundary transition separates two phases of Deccan volcanism at current well depths between 2500 m and 3500 m below the surface. The deep burial is due to the high sediment input and rapid subsidence after volcanism ended (e.g., Raju et al., 1995, 1996; Misra, 2005; Raju, 2008). In most wells, four phase 2 and three to four phase 3 megaflows are present and can be correlated across the basin based on lithology, biostratigraphy, and well log data (Fig. 9). These basalt megaflows are generally 5 m to 15 m thick, except for two wells, where phase 3 megaflows are 60 m thick (Fig. 9; CTP-A and RZL-A). Intertrappean sediments vary between 5 m and 15 m but occasionally reach 50 m (wells CTP-A, RZL-A). These anomalously thick basalt megaflows and intertrappean beds are likely due to infilling of local topographic lows. In contrast, near the paleoshoreline (Rajahmundry area), megaflows are stacked with no intertrappean sediments, except between Deccan phase 2 and phase 3 (Fig. 4C; Keller et al., 2008). Self et al. (2008) suggested that the overall pattern of the basalt megaflows is consistent with sheet flows of very large-volume pahoehoe flow fields.

Lithostratigraphy

Resistivity and gamma values show pronounced signals for the megaflows in all Krishna-Godavari Basin wells (Fig. 9), which are also correlated based on biostratigraphy (Fig. 3; Keller et al., 2011a). Resistivity for normal sandstones, siltstones, and shale varies between 1 and 6 Ωm, unless they are hydrocarbon bearing. In contrast, resistivity values for the basalts vary anywhere from 50 Ωm to >200 Ωm, depending on the amount of sediments incorporated as a result of erosion at the base and top of megaflows. In all Krishna-Godavari Basin wells, e-logs show high- to very high-resistivity peaks against the basalt flows, whereas some basalt beds are less distinct due to mixed sediments. Gamma logs show significantly lower values in basalt flows relative to the intertrappean clastic sediments (Fig. 9). The cores and drill cuttings from these megaflows are dark gray to green-gray in color, very hard, and compact.

Biostratigraphy

Planktic foraminiferal assemblages of the Krishna-Godavari Basin average between 20 and 30 species, which is typical diversity in middle neritic environments (Keller and Abramovich, 2009). Variations in species richness are due to preservation (dissolution effects) and availability of sample size, with cored intervals yielding the most reliable data (Fig. 10). Faunal assemblages below phase 2 megaflows are typical of zones CF1–CF3. In the absence of index species *Plummerita hantkeninoides* and

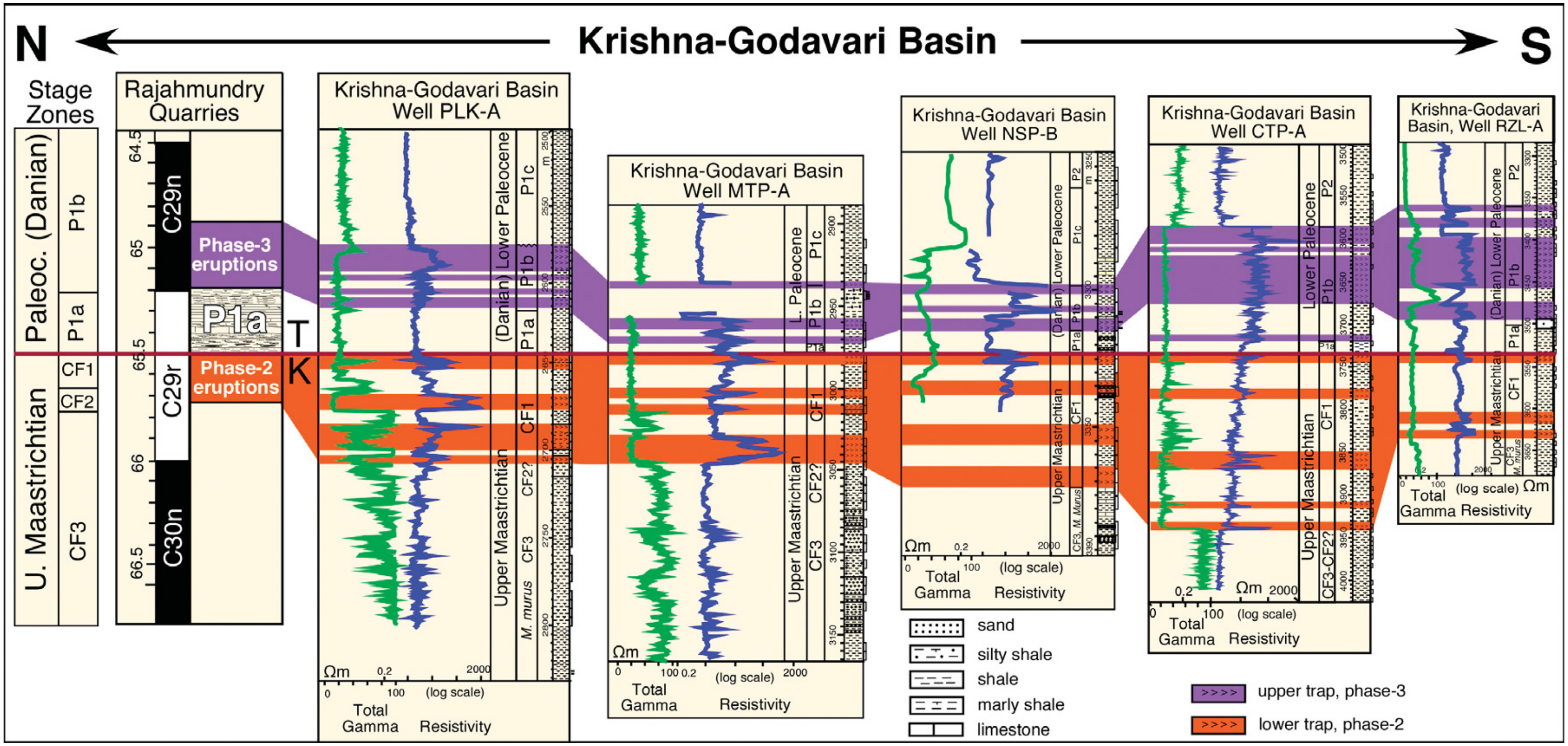

Figure 9. Correlation of Krishna-Godavari Basin wells based on biostratigraphy, Deccan lava megaflows, and well-log data (gamma and resistivity). Note that Deccan phase 2 and phase 3 each contains three to four basalt beds that represent Earth's longest megaflows. All megaflows are separated by relatively thin sandy (5–15 m) intertrappean beds. These megaflows correlate with the lower and upper traps in Rajahmundry quarries, where no intertrappean beds are present, except between phase 2 and phase 3 volcanic episodes (modified from Keller et al., 2011a). KTB—K-T boundary.

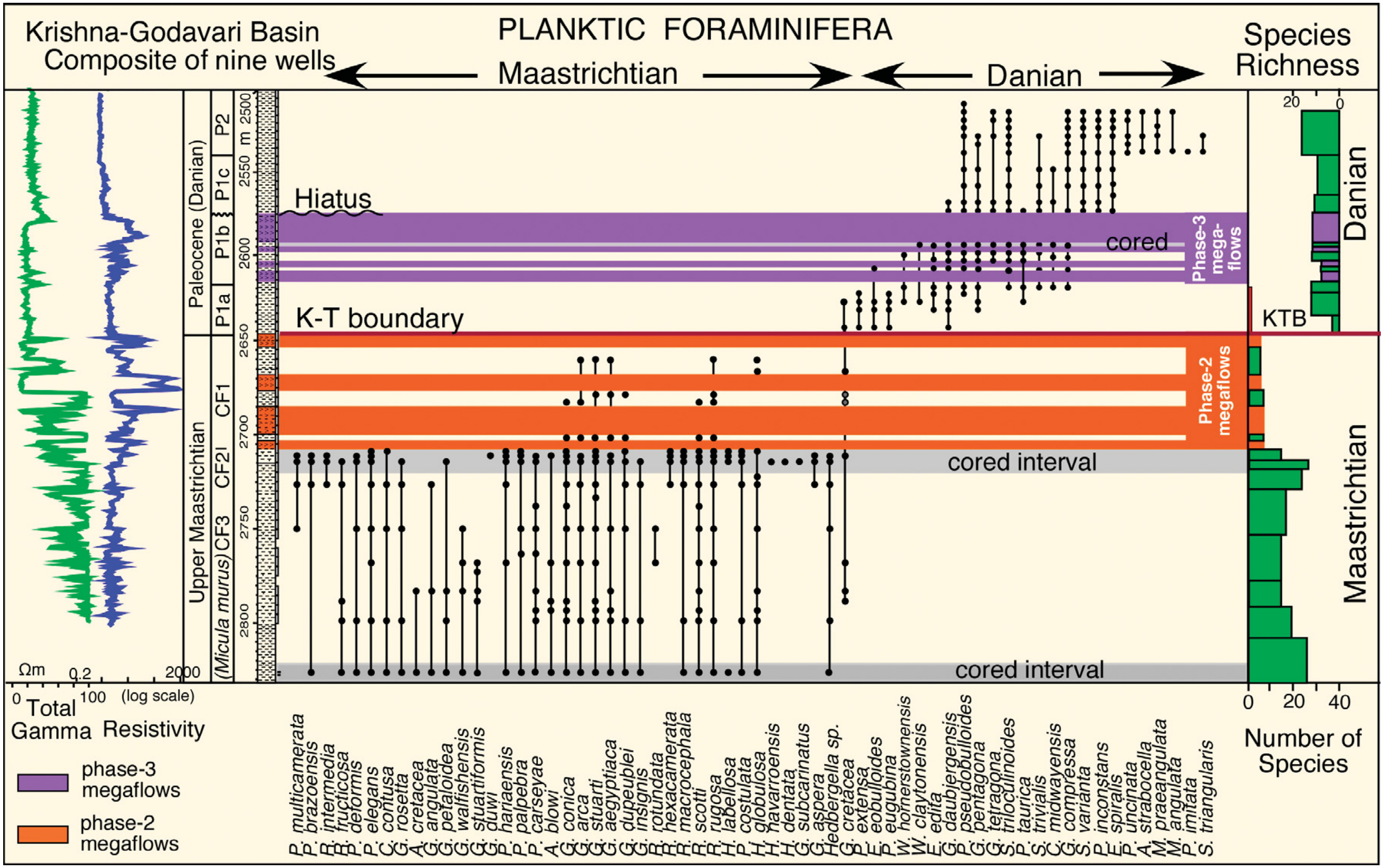

Figure 10. Composite species ranges of nine wells in the Krishna-Godavari Basin plotted against biostratigraphy and phase 2 and phase 3 lava flows of the PLK-A well. Gray shadings mark cored intervals that record the most reliable species richness data. Note the mass extinction began with 50% species extinctions before the first megaflow eruptions, followed by another 50% drop after the first megaflow, and was complete by the last megaflow at the K-T boundary. Figure is modified from Keller et al. (2011a).

Gansserina gansseri, these zones cannot be differentiated. However, zones CF1 and CF2 are nearly equivalent to the *Micula prinsii* nannofossil zone, and CF3 is nearly equivalent to the *Micula murus* zone, both of which have been identified in wells within and below phase 2 megaflows, respectively (Saxena and Misra, 1994, 1995; von Salis and Saxena, 1998).

Paleomagnetic and radiometric analyses place phase 2 megaflows in C29R below the K-T boundary (e.g., Knight et al., 2003, 2005; Chenet et al., 2007, 2008) correlative with zones CF1–CF2 and the *Micula prinsii* zone. Based on this correlation, Deccan phase 2 eruptions may span zones CF1–CF2, but the megaflows and intertrappean sediments of the Krishna-Godavari Basin were most likely deposited near the end of phase 2 and more specifically in zone CF1, which spans the last 160 k.y. of the Maastrichtian (Fig. 3). Based on magnetic analysis of individual lava flows, Chenet et al. (2007, 2008, 2009) and Courtillot and Fluteau (this volume) suggest that Deccan phase 2 may have occurred over as little as 100 k.y., with active eruptions over perhaps as little as 10 k.y. Possible support for such short-term deposition comes from Font et al. (2011), who identified low magnetic susceptibility in a short interval below the K-T boundary at Bidart, France, which they attributed to HCl-rich volcanic gas and aerosols derived from Deccan plumes. Based on sediment accumulation rates, this short interval marks the top 30,000 yr of zone CF1 at Bidart, where most planktic foraminifera are dissolved due to ocean acidification likely related to Deccan phase 2 (Font et al., this volume). If this interpretation is correct, then the most devastating effects of Deccan phase 2 volcanism were concentrated over a very short time interval at the end of the Maastrichtian.

Intertrappean sediments between phase 2 and phase 3 megaflows contain the earliest Danian zone P1a assemblage, similar to Meghalaya, Jhilmili, and Rajahmundry quarries (Figs. 5, 6, 8, and 10; Keller et al., 2008; Malarkodi et al., 2010). This demonstrates that the mass extinction of Cretaceous species was coeval with the underlying Deccan phase 2, suggesting a cause-effect relationship. Evolution of Danian species in the intertrappean sediments above phase 2 follows the same pattern as observed globally, with small, simple morphologies that reflect adaption for survival in highly stressed environments (e.g., Luciani, 2002; Coccioni and Luciani, 2006; Pardo and Keller, 2008). The fact that these early Danian assemblages mirror the global evolutionary pattern demonstrates that environmental conditions after the main Deccan phase 2 remained stressed in India and globally.

Phase 3 intertrappean assemblages are similar to zone P1a, except for the disappearance of the zone P1a index species *P. eugubina*, which indicates deposition in zone P1b (Fig. 3). Species remained dwarfed, and abundances of early zone P1a species decreased (e.g., *Parvularugoglobigerina extensa*, *Eoglobigerina edita*, *Woodringina claytonensis*, *Woodringina hornerstownensis*, *Eoglobigerina eobulloides*). This reflects continued high-stress conditions, as also observed globally (Pardo and Keller, 2008). After phase 3 volcanism, planktic foraminifera developed larger morphologies (>150 μm) and increased diversity globally (Fig. 10). Thus, the long delay in the global ecosystem recovery in the early Danian was likely due to climate change, increased weathering of Deccan basalts, and terrestrial runoff prolonging environmental stress conditions through P1a, followed by intense stress conditions associated with Deccan phase 3 (see Punekar et al., this volume).

Mass Extinction—Volcanic Phase 2

Results from nine deep wells analyzed in the Krishna-Godavari Basin provide strong evidence that the end-Cretaceous mass extinction was directly related to the main phase 2 of Deccan volcanism (Fig. 10). More specifically, we can conclude that this mass extinction began shortly before the eruption of the first of four megaflows that mark the world's largest and longest lava flows. A 4 m cored interval just below the first megaflow shows normal diversity near the base, followed by a rapid and permanent decrease in diversity of 50% toward the top of the core (Fig. 11; Keller et al., 2011a). Diversity and extinctions in intertrappean sediments, summarized based on nine wells (Fig. 10), show that another 50% species disappeared after the first megaflow, leaving just seven survivors. No recovery occurred between the next three megaflows, and the mass extinction of Cretaceous species was complete by the last megaflow at the K-T boundary.

This pattern of extinctions seems unequivocal in the rapid demise of planktic foraminifera. What is less clear is whether even the seven "survivors" were actually survivor species or simply reworked shells. Five of the seven species are thick-walled and robust globotruncanids, which globally tend to disappear early because of their environmental sensitivities. Their presence in the intertrappean may be an artifact of erosion and transport. Also uncertain is how rapid the four megaflow eruptions followed each other. Based on flow-by-flow magnetic stratigraphy, Courtillot and Fluteau (this volume) suggest that single eruptive Deccan events could have been emplaced in less than a decade (Chenet et al., 2009). The thickness of intertrappean sediments between the four megaflows generally ranges from 5 m to 15 m (Fig. 10), although occasionally wells with thicker deposits have been observed in the Krishna-Godavari Basin possibly due to topographic variations (Keller et al., 2011a). These intertrappean sediments are generally sandy and could have been deposited by either normal sedimentation over relatively short time intervals, or current transport from erosion of nearby topographic highs. In either case, deposition of the four megaflows and intertrappean sediments that mark the mass extinction just below the K-T boundary record a time interval possibly as short as a few thousand to tens of thousands of years.

Strong carbonate dissolution effects are observed in foraminifera from the intertrappean and infratrappean sediments of the Krishna-Godavari wells, as also noted in the Meghalaya section (Fig. 5). This indicates ocean acidification due to volcanic CO_2 and SO_2 resulting in decreased pH of ocean waters. Similar strong dissolution effects attributed to ocean acidification as a result of Deccan volcanism are also observed over a short interval (~30,000 yr) below the K-T boundary at Bidart, southern

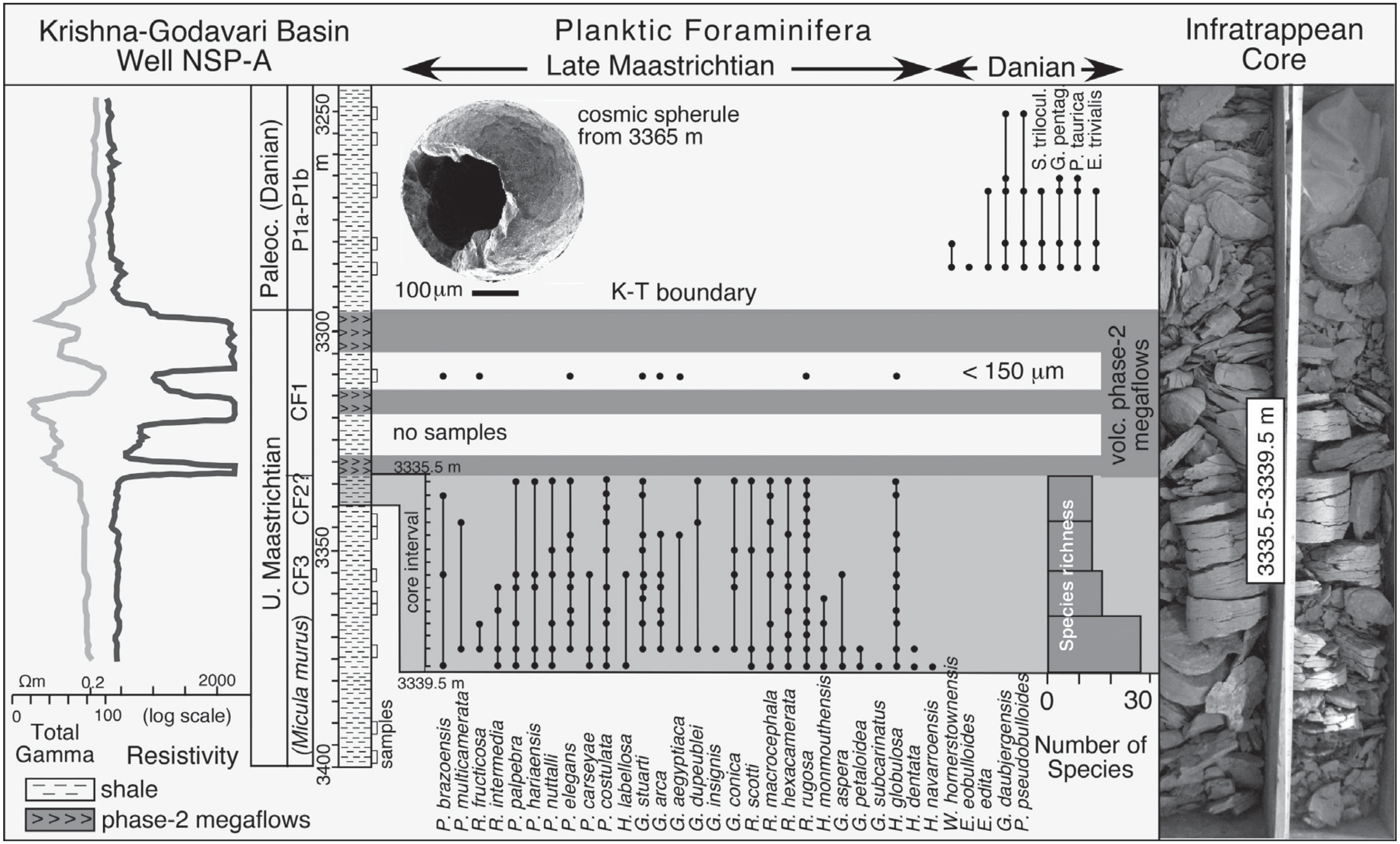

Figure 11. Onset of K-T boundary mass extinction in a 4 m core of India's Oil and Natural Gas Corporation (ONGC) well NSP-A. This core interval shows that 50% of the species disappeared prior to the first megaflow in the Krishna-Godavari Basin, which suggests active phase 2 volcanism in the main Deccan province prior to the megaflows that reached Rajahmundry and ended with the mass extinction of nearly all planktic foraminifera. A cosmic spherule was found 25.5 m below the cored interval, though its significance is unclear (from Keller et al., 2011a).

France (Font et al., 2011). Dissolution effects below the K-T boundary mass extinction are well known but have garnered little attention to date because their cause remained a mystery. A systematic survey remains to be done to evaluate this potential link to Deccan volcanism.

How rapid was this mass extinction? In deep-sea sections globally, the mass extinction occurred over a very short time interval, which in condensed sections appears instantaneous. This is perhaps the main reason an instantaneous extraterrestrial cause for the mass extinction is the preferred interpretation by many scientists. Large igneous eruptions such as the Deccan Traps, Siberian Traps, and the Central Atlantic magmatic province are commonly believed to have occurred over one or more million years. This perception is erroneous, and better dating techniques (U-Pb) for Central Atlantic magmatic province volcanism reveal a rapid mass extinction associated with the first major eruption pulse lasting just a few tens of thousands of years (Blackburn et al., 2013). Other indicators for voluminous short-duration eruptions come from weathering rates, red bole layers, absence of intertrappean sediments in the Deccan Traps, and flow-by-flow magnetic stratigraphy (Chenet et al., 2007, 2008; Courtillot and Fluteau, this vol). Absolute dating of Deccan basalt flows by U-Pb methods similar to that conducted for the Central Atlantic magmatic province still remains to be done.

Climatic and Environmental Effects of Deccan Volcanism

Upper Maastrichtian to early Danian paleoclimatic effects of Deccan volcanism can be assessed based on the chemical index of alteration (CIA), which is commonly used to estimate the intensity of weathering related to climatic conditions (Nesbitt and Young, 1982, 1989). Late Maastrichtian CIA values of zone CF3 are relatively high (mean 69), indicating dry seasonal conditions (Fig. 12). In the 4 m of infratrappean sediments below the first phase 2 megaflows, CIA values gradually decrease (mean 62). This suggests that significant volcanic activity had initiated well before the first megaflows in the Krishna-Godavari Basin. During this time, climate turned increasingly arid, correlative with the onset of the mass extinction in planktic foraminifera.

Minimum CIA values (mean 53) are reached in the intertrappean sediments of phase 2 (zone CF1) and in the earliest Danian intertrappean sediments (zone P1a; Fig. 12), which indicates arid conditions. In the uppermost interval of phase 3 (zone P1b), CIA values (mean 76) are similar to those measured in sediments below phase 1 volcanism of the early late Maastrichtian (Keller et al., 2012). This suggests a return to more humid conditions, possibly linked to reduced or intermittent volcanic activity.

Similar arid to semiarid conditions with seasonal wet and dry cycles have been observed in smectite-enriched paleosols of the early Danian intertrappean sediments between volcanic phase 2 and phase 3 at Rajahmundry and Jhilmili (Keller et al., 2008, 2009a), in intertrappean sediments at Anjar, Kutch, close to the Deccan volcanic province (Khadkikar et al., 1999), and in Meghalaya, 800 km from the Deccan volcanic province (Gertsch et al., 2011a). Localized arid conditions surrounding the Deccan volcanic province are interpreted as "mock aridity" resulting from volcanically induced xeric conditions and extreme geochemical alkalinity in a regionally more humid climate (Harris and Van Couvering, 1995; Khadkikar et al., 1999; Gertsch et al., 2011a).

Na/K and K/(Fe + Mg) ratios reveal the balance between detrital and volcanogenic input, which may also reflect climate conditions (Gertsch et al., 2011a; Keller et al., 2012). In the late Maastrichtian zones CF3 and CF2–CF1 (intervals A and B), below phase 2 megaflows (Fig. 12), sediments show steady Na/K ratios close to mean shale values, whereas K/(Fe + Mg) ratios are closer to mean Deccan basalt values. In the latest Maastrichtian zone CF1 and early Danian zone P1a (intervals C and D), these ratios reflect a dominant basaltic source consistent with deposition of the main phase 2 megaflows in zone CF1. In the early Danian phase 3 megaflows (interval E), Na/K decouples from K(Fe + Mg) ratios, which may reflect increasing humidity, as suggested by the CIA index, and increased weathering of Fe-Mg–enriched minerals.

Additional information can be gained from weathering of basalts. During the early late Maastrichtian (zone CF3, interval A), the Ca/Na and Mg/Na ratios are stable and close to mean shale values, typical for rivers draining silicate rocks, such as granite, gneiss, and shale (Gertsch et al., 2011a). However, just below the onset of phase 2 megaflows (interval B), both proxies reach values normally recorded in basaltic river waters (Dessert et al., 2003). These variations are interpreted to result from chemical weathering of Ca- and Mg-rich volcanic rocks (Fig. 12). This suggests that the Krishna-Godavari Basin was part of the drainage of the Deccan volcanic province and that significant basalt outcrops were already present prior to phase 2 megaflows. Surprisingly, both ratios decrease considerably in the CF1 intertrappean sediments of phase 2, especially in the lower part, suggesting reduced weathering of basalt linked to the increased aridity (mock aridity) evident in the CIA proxy (Fig. 12). During phase 3, increased ratios reflect a return to more humid conditions and enhanced weathering.

HIGH-STRESS ENVIRONMENTS: *GUEMBELITRIA* BLOOMS

Guembelitria blooms are well-known indicators of high-stress environments first documented in the aftermath of the K-T boundary mass extinction, notably in the Tunisian sections of El Kef and Elles and subsequently worldwide (review in Keller and Pardo, 2004). More recently, *Guembelitria* blooms were also documented in the latest Maastrichtian zone CF1 marking high-stress conditions in the ~160,000 k.y. preceding the K-T boundary mass extinction (review in Pardo and Keller, 2008), during the early late Maastrichtian C30n (67.4 Ma), and early Danian C29n (review in Punekar et al., this volume). These three bloom intervals correlate with the three main phases of Deccan volcanism and climate warming (Fig. 13).

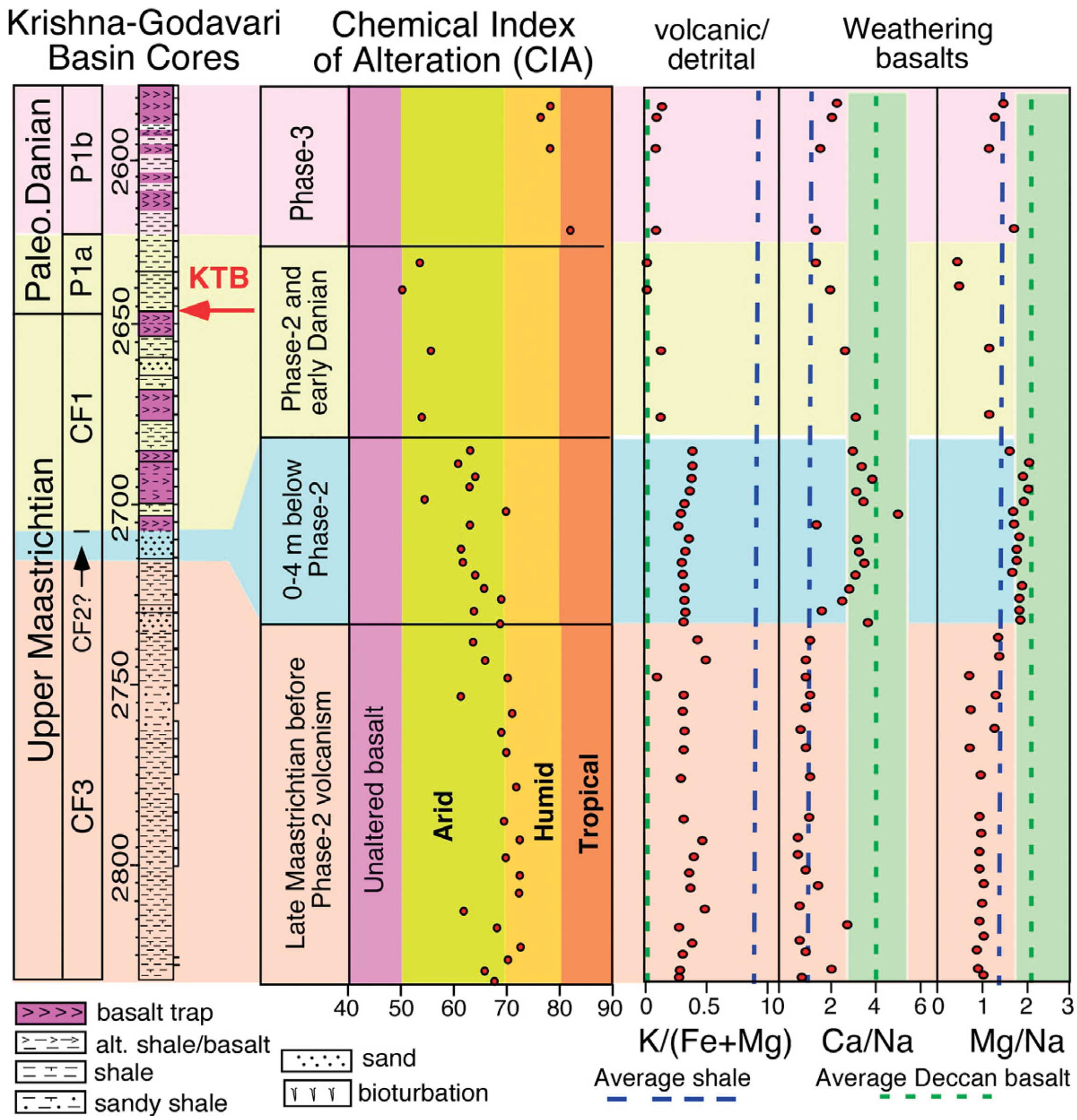

Figure 12. Geochemical proxies of volcanism (weathering of basalt, volcanism vs. detritism) and the chemical index of alteration (CIA) based on major-element geochemistry. Note the change in the weathering index and CIA from humid to arid with the onset of Deccan main phase 2 in the late Maastrichtian and the return to normal humid tropical conditions after the last Deccan phase 3 in the early Danian. Blue dashed line—mean average shale (Wedepohl, 1971); green dashed line—Deccan mean average basalt (Crocket and Paul, 2004); green shaded field—range of Deccan basalt river values (Dessert et al., 2003); KTB—K-T boundary. Figure is modified from Keller et al. (2012).

Phase 2 Volcanism

In Meghalaya, India, *Guembelitria* blooms reach 95% of the foraminiferal population coincident with Deccan phase 2, which indicates high environmental stress as a direct result of Deccan volcanism (Fig. 5). In addition, the giant test size of *Guembelitria* suggests superstress conditions surrounding the Deccan volcanic province. The large *Guembelitria* test size appears to be indirectly related to Deccan volcanism–induced climate warming and associated effects. On the basis of mineralogical, geochemical, and trace-element analyses of the Meghalaya (Um Sohryngkew) section, Gertsch et al. (2011a) argued that intense physical and chemical weathering of the continental areas was likely due to acid rains as a result of high SO_2 emissions during the latest Maastrichtian when Deccan phase 2 volcanic activity reached its maximum (Self et al., 2006). During this time, high terrestrial influx of silt and nutrients led to eutrophication and muddy waters, which resulted in reduced penetration of sunlight

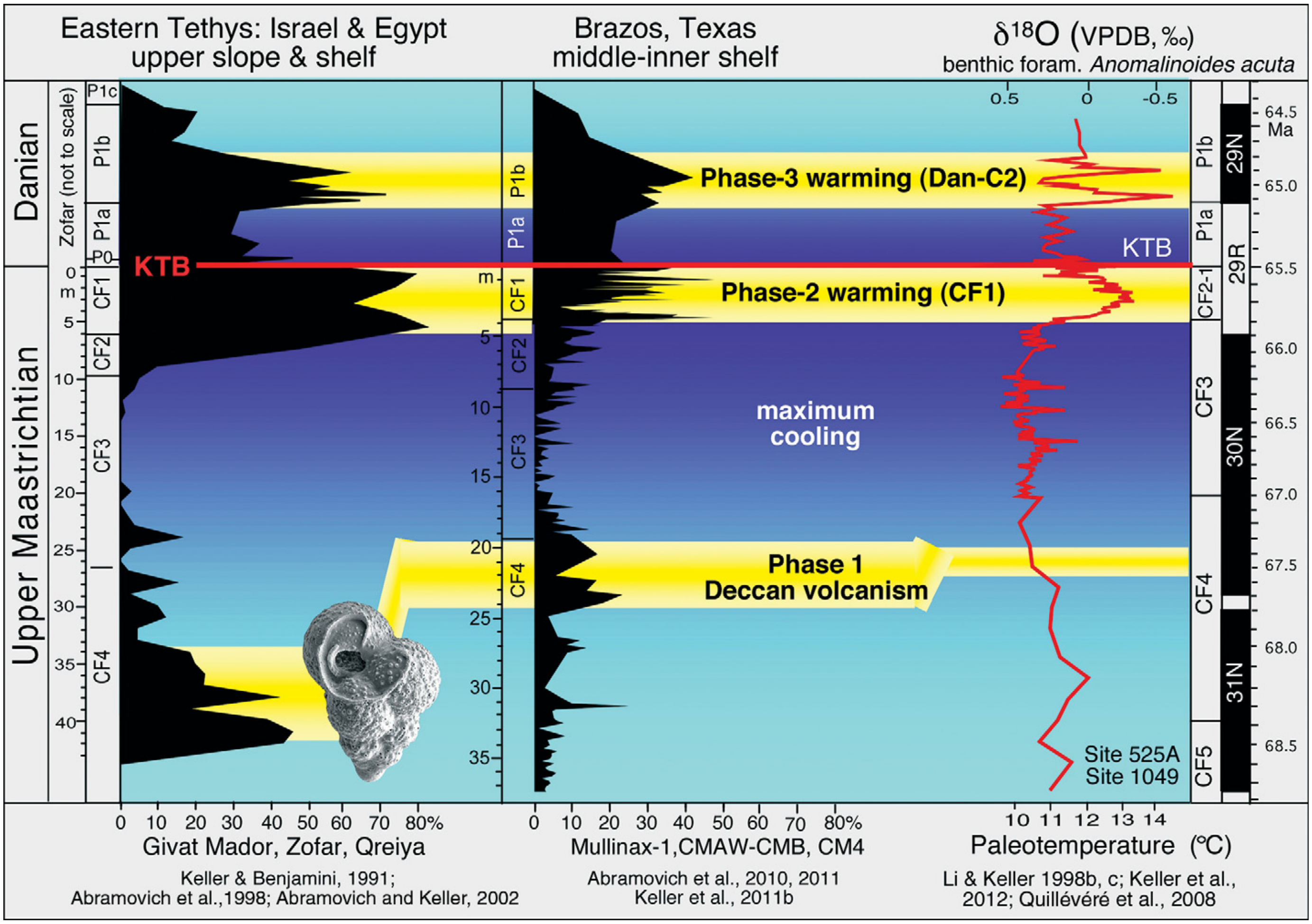

Figure 13. *Guembelitria cretacea* blooms recorded from the eastern Tethys and Texas correlative with the three phases of Deccan volcanism. Deccan phase 2 and phase 3 are associated with times of rapid warming in zones CF1 and P1b. Insufficient data are available to evaluate the environmental effects of the initial volcanic phase 1. KTB—K-T boundary; VPDB—Vienna Peedee belemnite. Stable isotope data are from Li and Keller (1998c) and Quillévéré et al. (2008). Faunal data are from Keller and Benjamini (1991), Keller et al. (2011b), and Abramovich et al. (2011).

in the shallow Um Sohryngkew area. Similar volcanism-induced climate change and resultant high physical and chemical erosion leading to high ecosystem stress were inferred for the Permian-Triassic boundary mass extinction (Algeo and Twitchett, 2010).

At the K-T boundary in Meghalaya, *Guembelitria cretacea* may have adapted to these high-stress conditions by inflating chambers, resulting in higher buoyancy to live near the water-atmosphere interface. Acidic ocean waters inhibited $CaCO_3$ production, particularly of thicker-shelled larger species living in subsurface water, which favored blooms of the thin-shelled *Guembelitria*, the only species dwelling in the uppermost surface waters (Abramovich et al., 2010). This may explain the near absence of all other species, which account for only 2%–5% of the total foraminiferal population during this time (Fig. 5). *Guembelitria* blooms, though not the morphologic gigantism, have been observed throughout the Tethys, and Atlantic and Indian Oceans (e.g., Pardo and Keller, 2008; Keller and Abramovich, 2009). *Guembelitria* blooms are thus excellent indicators of high-stress environments particularly related to Deccan volcanism.

Phase 3 Volcanism—Delayed Biotic Recovery

Guembelitria blooms prevailed in the aftermath of the K-T boundary mass extinction worldwide, reflecting the continued high-stress environment in the early Danian zones P0 and P1a, but they decreased in the upper part (P1a[2]), suggesting incipient recovery (Pardo and Keller, 2008). Throughout this time, species diversity is very low (<12 species), characterized by simple species morphology and dwarfed size (<63 µm; Keller and Abramovich, 2009). However, in zone P1b, correlative with phase 3 volcanism, large *Guembelitria* blooms reappear, marking the return to higher-stress conditions.

The last phase 3 of Deccan volcanism began near the base of C29N, with the largest eruptions resulting in three to four megaflows in the Krishna-Godavari Basin (Knight et al., 2003, 2005; Baksi, 2005; Jay and Widdowson, 2008; Jay et al., 2009). Intertrappean sediments contain typical early Danian zone P1b foraminiferal assemblages dominated by *Guembelitria cretacea*, *Globoconusa daubjergensis*, and biserial species, which are observed globally (Punekar et al., this volume), and species sizes remained small (generally <100 µm; review in Keller and Abramovich, 2009). In India, no major differences are observed between faunal assemblages of the three intertrappean layers, and only a few earlier Danian species disappeared (e.g., *Parvularugoglobigerina eugubina*, *Parvularugoglobigerina longiapertura*). This suggests that high-stress environmental conditions persisted but that sufficient time elapsed between eruptions to permit environmental recovery, thus avoiding the extinctions evident in volcanic phase 2. Alternatively, these early Danian species, which evolved during high-stress conditions, may have been primed for survival, unlike the highly specialized species of the late Maastrichtian. Similar to volcanic phase 2, *Guembelitria* blooms of phase 3 are observed through the Tethys (Fig. 13; see also Punekar et al., this volume), indicating global high-stress environments but with less severe conditions than during Deccan phase 2. The age and duration of phase 3 volcanism cannot be estimated based on current data.

Full recovery in marine plankton after the K-T boundary mass extinction occurs in zone P1c, well after Deccan phase 3 and the Dan-C2 global warm event commonly associated with this volcanic event (Fig. 13; Quillévére et al., 2008), when diversity, species size, and species complexity increased in India and globally (Keller and Abramovich, 2009; Keller et al., 2011a; Punekar et al., this volume). The coincidence of planktic foraminiferal recovery, and by extension ecosystem recovery, with the last phase of Deccan volcanism suggests that the long delayed recovery after the mass extinction was likely due to Deccan volcanism.

CHICXULUB IMPACT—LINKED TO MASS EXTINCTION?

The Chicxulub impact on Yucatan is commonly assumed to have caused the K-T boundary mass extinction. This interpretation was sanctified by the redefinition of the K-T boundary as impact ejecta associated with the mass extinction (Gradstein et al., 2004; Molina et al., 2006; Arenillas et al., 2006; Schulte et al., 2010). The problem with defining Chicxulub impact ejecta as K-T boundary in age is not just circular reasoning, but that it has actually prevented establishing the true age of this impact (Keller, 2011). Many researchers simply ignored the stratigraphic position of impact ejecta (impact glass spherules, Ir enrichments), unless positioned at or near the K-T boundary, which is considered the ultimate proof of Chicxulub's K-T boundary age. The many localities with older and younger impact spherule layers are ignored or dismissed with ad hoc explanations lacking evidence (Schulte et al., 2010). The age of the Chicxulub impact is the main basis for the decades of controversy. A brief review of the Chicxulub impact spherule evidence reveals this age problem.

North Atlantic, Caribbean, Central America

The biostratigraphic position of impact spherule layers of all known K-T boundary sequences is well known and illustrated in Figure 14. The age distribution pattern is complex, revealing multiple spherule layers and systematic reworking. Throughout the North Atlantic, Caribbean, Haiti, Cuba, Belize, Guatemala, and southern Mexico, multiple impact spherule layers are reworked in early Danian zone P1a sediments above an unconformity that spans the K-T boundary (Fig. 3; reviews in Keller et al., 2003a, 2003b). In a few localities of the North Atlantic and Caribbean, a single thin (2 cm to 15 cm) spherule layer overlies Maastrichtian sediments (e.g., Bass River, New Jersey, Ocean Drilling Program [ODP] Sites 999B, 1001B, 1049A–C, and 1259B) and has been hailed as the ultimate proof that the Chicxulub impact is K-T boundary in age (Olsson et al., 1997; Norris et al., 1999, 2000; MacLeod et al., 2007). This is the main basis for the redefinition of Chicxulub as K-T boundary age (Schulte et al., 2010).

Recent high-resolution stable isotope and quantitative planktic foraminiferal analyses of these sections reveal a K-T boundary hiatus that spans from the late Maastrichtian zones CF1–CF2 and sometimes also CF3 (NJ Bass River) through the early Danian zones P0 and most of P1a(1) (Keller et al., 2013). Moreover, impact spherules are reworked in early Danian sediments (upper zone Pla[1]) as indicated by abundant *Parvarugoglobigerina eugubina* and diverse Danian assemblages of up to 12 species, most of which do not evolve until ~100 k.y. after the K-T boundary. Despite the abundance of *P. eugubina* in the spherule layer of ODP Site 1049, previous investigators claimed that this species first appeared immediately above the spherule layer, indicating spherule deposition at the K-T boundary (Olsson et al., 1997; Norris et al., 1999, 2000). Despite the absence of zone CF1 (ODP Site 1049, New Jersey Bass River core), they claimed that the K-T boundary is complete, attributing the absence of the index species *Plummerita hantkeninoides* to environmental exclusion, although this species has been reported from Spain as well as ODP Site 1259 (Pardo et al., 1996; MacLeod et al., 2007). Recently, Schulte et al. (2010) hailed these NW Atlantic localities as proof that Chicxulub is K-T boundary in age. Given the fragmented record of the North Atlantic and Caribbean, as a result of the ancient Gulf Stream and complex tectonic activity (Fig. 14; Keller et al., 1993, 2013; Watkins and Self-Trail, 2005), this area is unlikely to yield complete sediment records across the K-T boundary. Such records are most likely obtained from NE Mexico and Texas.

NE Mexico and Texas

Impact Tsunami or Long-Term Deposition?

Throughout NE Mexico and along the Brazos River, Texas, dozens of outcrops reveal multiple impact spherule layers in sediments of zone CF1 that spans the last 160 k.y. of the Maastrichtian. These spherule layers are generally at the base of submarine channels and contain mixed shallow-water debris from nearshore

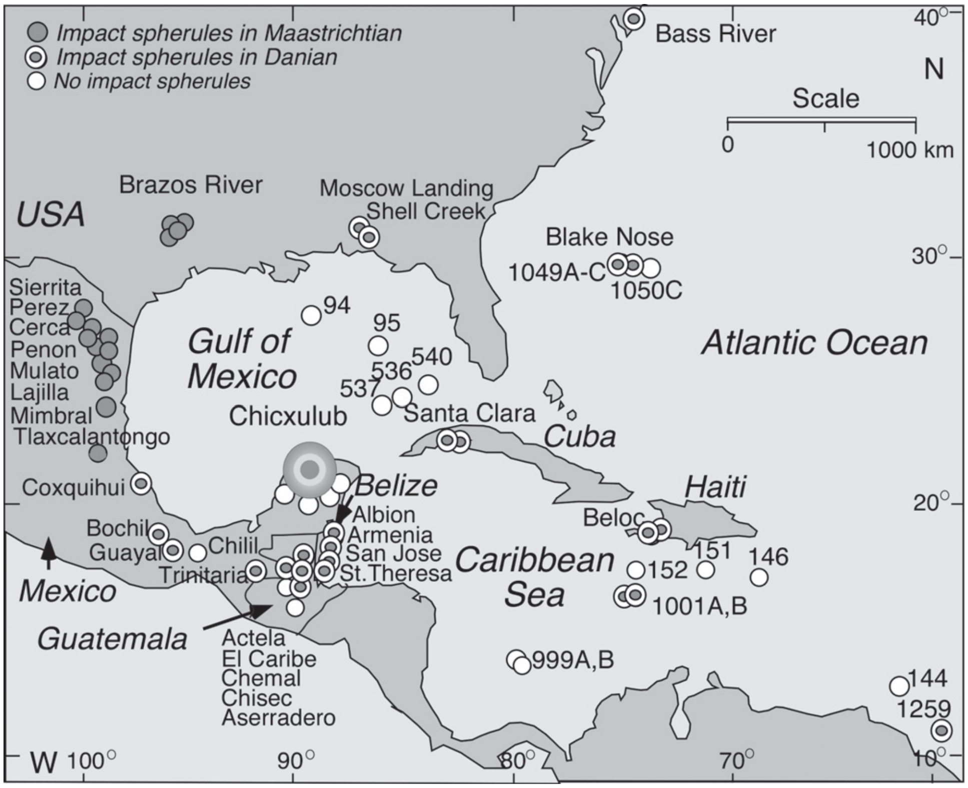

Figure 14. K-T boundary localities with impact spherules surrounding the Chicxulub impact crater on Yucatan with stratigraphic positions of impact spherules. Note that impact spherule layers in NE Mexico and Texas are in zone CF1, which spans the last 160 k.y. of the Maastrichtian. In all other localities, impact spherule layers are reworked in early Danian sediments of zone P1a(1) (lower part of *Parvularugoglobigerina eugubina* zone) and frequently overlie a hiatus at the K-T boundary.

areas (plant remains, shallow-water benthic foraminifera, glauconite) transported via submarine channels to depths between 500 and 1000 m in NE Mexico (Fig. 15; Adatte et al., 1996; Keller et al., 1997, 2002b, 2003a; Alegret et al., 2001; Schulte et al., 2003). Along the Brazos River, deposition occurred in a shallow middle to inner neritic environment (Keller et al., 2011b; Hart et al., 2011). In NE Mexico localities, additional impact spherule layers are present in marls and marly limestone several meters below the channel deposits (Fig. 15).

Clues to the depositional nature of these submarine channel deposits come from sedimentary features. In NE Mexico, two spherule layers at the base of the channel are separated by a 20 cm thick sandy limestone layer (e.g., El Mimbral, El Peñon, La Lajilla) and by sandstone layers in the Brazos sections (Keller et al., 2011b; Adatte et al., 2011). The limestone layer at El Peñon contains rare truncated J-shaped burrows infilled with spherules (Figs. 16A and 16B). Similar spherule-filled truncated burrows are observed near the base of the overlying sandstone unit (Keller et al., 1997; Ekdale and Stinnesbeck, 1998). The top unit of this channel deposit consists of alternating fine sand and laminated shale layers with multiple horizons of bioturbation by *Chondrites*, *Planolites*, *Ophiomorpha*, and *Zoophycos* (Ekdale and Stinnesbeck, 1998), and similar burrowed horizons are reported from the Brazos sections (Gale, 2006). Two discrete zeolite layers have been traced in the sandstone units across NE Mexico (Adatte et al., 1996). In addition, there are the thick impact spherule layers 4–9 m below the submarine channel deposits. All of these sedimentary features require long-term deposition.

However, deposition via impact-generated tsunami waves is the most common interpretation of these deposits because of the presence of impact spherules and their link to Chicxulub (e.g., Bourgeois et al., 1988; Smit et al., 1992, 1996; Heymann et al., 1998; Arenillas et al., 2006; Hart et al., 2011; Schulte et al., 2003, 2006, 2010). In this scenario, the sandy limestone between spherule layers is interpreted as large-scale tectonic disturbance (none has been documented), the J-shaped spherule-filled burrows are fluid-escape structures, the bioturbated horizons do not exist or are the result of downward burrowing from the K-T boundary, and the spherule layers below the K-T boundary were caused by tsunami and earthquake disturbance or liquefaction. They conclude, "A range of sedimentary structures and lack of evidence for ocean floor colonization within the clastic unit in northeastern Mexico indicate rapid deposition" (Schulte et al., 2010, p. 1215).

A more parsimonious interpretation compatible with the evidence is long-term deposition via normal sedimentation processes during a low sea level and subsequent rise, as documented from sections in NE Mexico and Texas (Adatte et al., 1996, 2011). In this scenario, impact spherules were eroded in nearshore environments at repeated intervals (explains shallow-water debris and multiple spherule layers) and transported via submarine channels into deeper water. More massive sandstone above the spherules may represent normal gravity flows or slumps along the slope of the Gulf of Mexico. The fine sand and laminated shale alternation

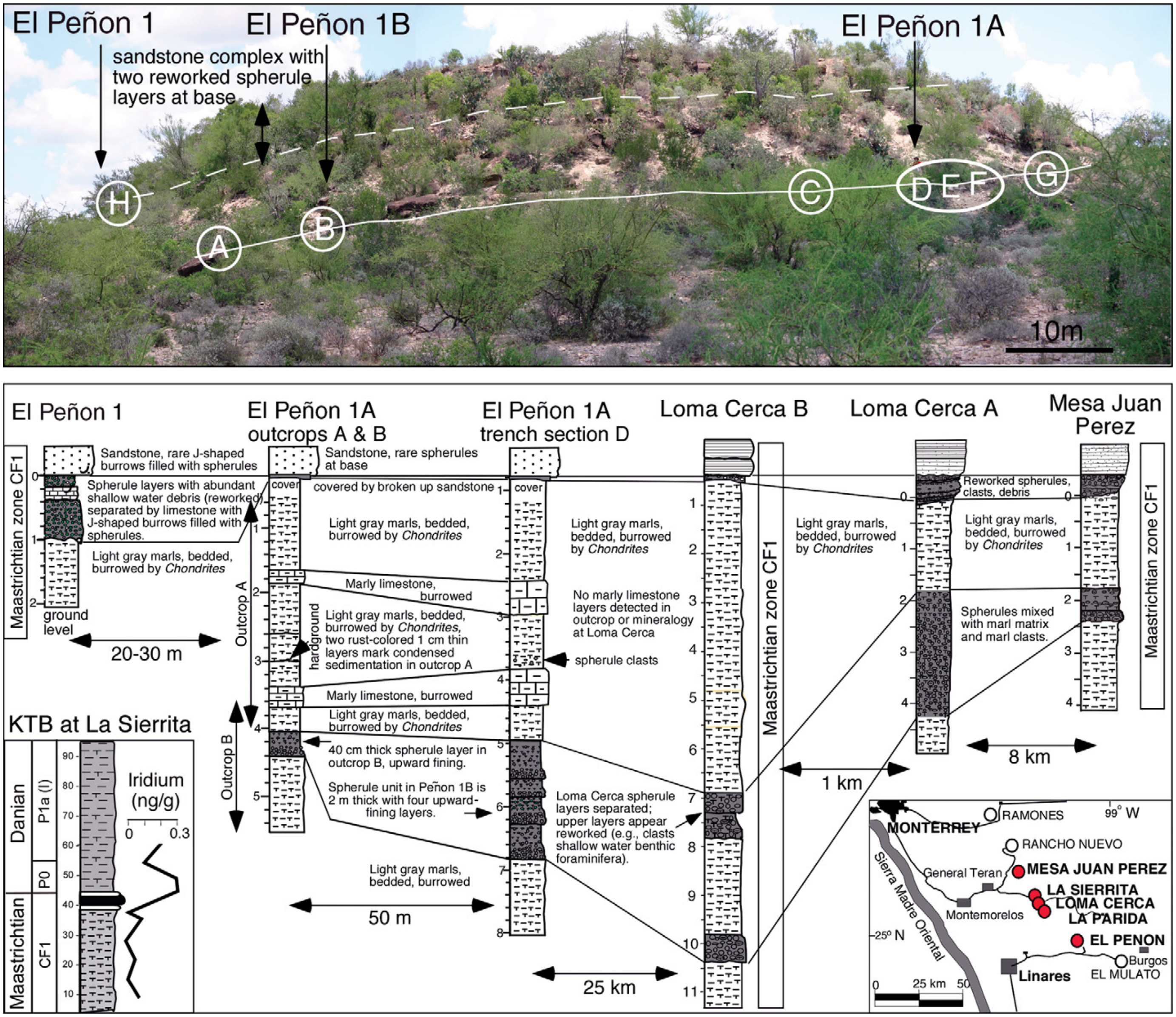

Figure 15. Photo showing sequence of El Peñon outcrops and associated stratigraphic logs. Dashed line in photo traces the sandstone complex with reworked impact spherules at the base of a submarine channel; solid line 4–5 m below traces the impact spherule layer near the base of zone CF1, with an estimated age 100–150 k.y. below the K-T boundary. El Peñon spherule layers can be correlated to Loma Cerca and Mesa Juan Perez sections at 25 km and 35 km to the north, respectively. Variable erosion in submarine channels below the reworked spherule unit at the top accounts for the reduced marl layers at Loma Cerca A and Mesa Juan Perez. The K-T boundary (KTB) is exposed at La Sierrita and contains no evidence of Chicxulub impact spherules (modified from Keller et al., 2009d).

represents the rising sea level and return to normal sedimentation along with colonization of the seafloor by invertebrates (e.g., Adatte et al., 1996, 2011; Ekdale and Stinnesbeck, 1998; Keller et al., 1997, 2007, 2011b; Gale, 2006).

Oldest Impact Spherule Layer

The age of the Chicxulub impact is best evaluated based on the stratigraphic position of the oldest impact glass spherule layer (Keller, 2008). At Loma Cerca, the stratigraphically oldest spherule layer was discovered 9 m below the channel deposits (Fig. 15; Keller et al., 2002b) and was interpreted by Schulte et al. (2003) as slump or tectonic disturbance. However, the only evidence of disturbance is a small (<2 m) overturned gravity flow within a spherule layer sandwiched between more resistant marl layers along a slope at Loma Cerca.

During a Princeton undergraduate student field trip in 2002, we tested the hypothesis that a stratigraphically older spherule layer should be present below the reworked spherule layers of

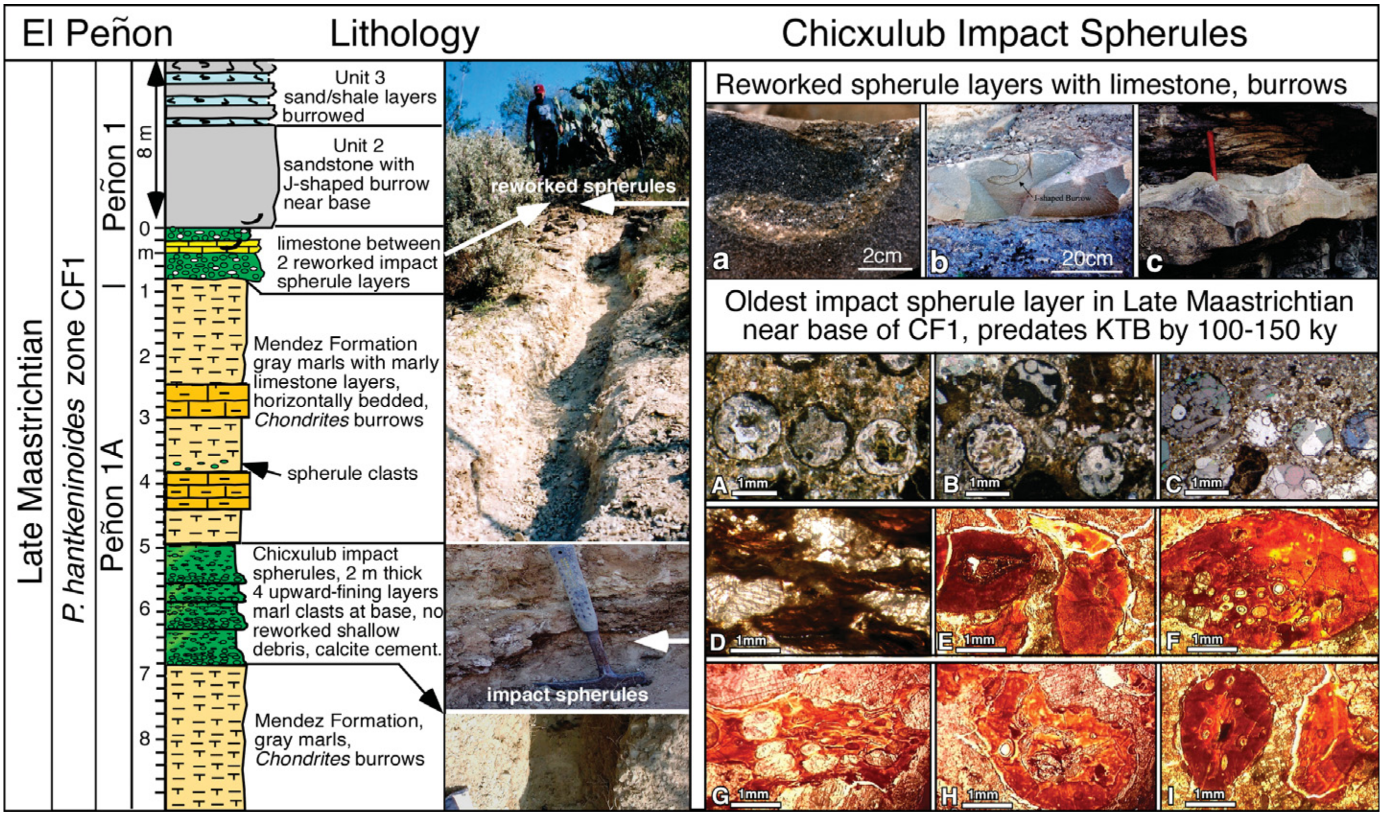

Figure 16. Composite section of the sandstone complex at El Peñon 1 and underlying trenched sequence at El Peñon 1A ~100 m southwest. At El Peñon 1A, sediments consist of horizontally bedded marls with two marly limestone layers and an impact spherule layer 4 m below the two reworked spherule layers at the base of the sandstone complex (dashed line). Peñon 1: (a) J-shaped burrow infilled with spherules and truncated from limestone (b) located between two reworked impact spherule layers, and (c) limestone layer with sculpted top between impact spherule layers at El Mimbral. Peñon 1A: A–B—Chicxulub impact spherules in marly matrix from the upper part of the 2-m-thick spherule unit; C—contact to overlying marl. D—melt-rock glass of welded spherules; E—spherules, some with concave-convex contact; F, I—compressed, vesicular spherules; G—vesicular glass shard; H—dumbbell. Deposition of this impact spherule layer occurred rapidly, possibly by raft-like accumulation of hot spherules at the sea surface and rapid sinking. KTB—K-T boundary.

the submarine channel at El Peñon. A trench was dug on the backside of the hill (Fig. 16; El Peñon 1A, location D). About 4–5 m below the base of the sandstone complex, a 2-m-thick impact spherule layer was discovered interbedded in undisturbed marls and marly limestones, thus confirming the hypothesis of an older pre–K-T boundary age for the Chicxulub impact. Subsequently, this older spherule layer was traced over ~100 m to El Peñon 1 (outcrop H) where strata dip below base level. Over the exposed distance, the spherule layer thins to 10–20 cm but remains parallel to the sandstone complex above (Fig. 15, dashed line). The 4–5 m of sediments consist of nearly horizontally layered marls and marly limestone with no signs of slumps, gravity flows, or tectonic disturbance (Keller et al., 2009d). This stratigraphically older spherule layer is near the base of zone CF1, similar to the oldest spherule layers at Loma Cerca and Mesa Juan Perez (Fig. 15; Keller et al., 2002b).

Nature of spherule deposition. Clues to the age and depositional nature of this spherule deposit can be gained from the spherules and matrix composition (Fig. 16; Keller et al., 2009d). A composite section based on El Peñon 1 and 1A shows the stratigraphy and deposition of the entire sequence in zone CF1, which spans the last 160 k.y. of the late Maastrichtian below the K-T boundary (Fig. 16). At the base, the spherule layer overlies an erosional surface with angular and rounded (2–5 cm, occasionally 10–20 cm) rip-up clasts from the underlying marls. Rip-up clasts decrease in abundance and size up section. The 2-m-thick spherule layer consists of four sublayers with upward-decreasing spherule abundance.

At the base, the more densely packed impact glass spherules form 5–10-cm-thick resistant layers of impact glass, and compressed and welded spherules, which are often amalgamated (Fig. 16D). Spherules are relatively large (2–5 mm), frequently compressed, oval (Figs. 16F and 16I), and dumbbell (Fig. 16H) vesicular, and some have concave/convex contacts (Fig. 16E). Vesicular glass shards are relatively common (Fig. 16G). The matrix is 80%–90% calcite with almost no clastic grains. Foraminifera are generally absent, except occasionally encased in glass (Keller et al., 2009d). In the upper parts of the unit, spherules are smaller and isolated in a marly matrix (Figs. 16A–16B). Above the spherule unit, the contact with the overlying marls is gradational (Fig. 16C) and bioturbated with diverse foraminiferal assemblages. Marls below the spherule layers are similar to those above (Keller et al., 2009d).

These spherule characteristics, including the distinct layers of welded glass, calcite cement, and near absence of detritus, indicate rapid settling of spherules through the water column. The welded glass rafts suggest that hot impact glass spherules accumulated at the sea surface before rapidly sinking to the seafloor. Abundant burrows in the marls and the gradational contact above the spherule unit reflect normal pelagic sedimentation after deposition of the spherule unit. Absence of exotic clasts and transported shallow-water debris indicates locally derived sediments. All these characteristics suggest that the late Maastrichtian spherule unit at El Peñon records the time of the Chicxulub impact.

Evidence from Brazos River, Texas. A pre–K-T boundary spherule age is also documented in the Brazos sections, where the K-T boundary mass extinction and evolution of Danian species occur up to 1 m above the sandstone complex of shallow submarine channels. Impact spherules, glauconite, and shell debris form an unconsolidated unit with rare lithified clasts at the base. Thin sections of the lithified clasts reveal the presence of impact spherules, and some clasts have burrows infilled with spherules (Keller et al., 2007, 2011b; Adatte et al., 2011). These spherule-rich clasts record a history of prior deposition, lithification, erosion, transport, and redeposition. Their age therefore predates the K-T boundary and also spherule deposition at the base of the channel. A yellow clay layer 45–60 cm below the channel unconformity was earlier thought to represent altered impact glass, but it has now been identified as a bentonite layer (Keller et al., 2011b; Adatte et al., 2011; Hart et al., 2012). Note that in the Brazos sections, Schulte et al. (2006) and Hart et al. (2011) place the K-T boundary at the spherule layer based on the redefinition of Chicxulub impact spherules as K-T boundary age, a practice that defies the primary K-T boundary identifying criteria—the mass extinction and evolution of Danian species up to 1 m above the top of the sandstone complex.

Evidence from the Chicxulub impact crater. A pre–K-T boundary age for the Chicxulub impact was also documented in the impact crater core Yaxcopoil-1 (Keller et al., 2004a, 2004b) and in two nearby Pemex cores (Ward et al., 1995). In the Yaxcopoil-1 core, the impact breccia (suevite) is separated from the K-T boundary by 50 cm of limestone with five glauconite clay layers, common burrows, a planktic foraminiferal assemblage of zone CF1, characteristic late Maastrichtian stable isotope values, and paleomagnetic chron 29r. Based on all these late Maastrichtian indicators, the age of the Chicxulub impact occurred sometime in zone CF1, preceding the K-T boundary mass extinction. Smit et al. (2004) argued that the 50 cm section of limestone represents backwash from the impact-generated tsunami and that the reported planktic foraminifera are just dolomite rhombs. Arz et al. (2004) and M. Caron (at the request of Smit) confirmed the presence of planktic foraminifera.

Probable age of Chicxulub impact. We can estimate the probable pre–Cretaceous boundary age of the Chicxulub impact based on Texas, NE Mexico, and the Chixculub crater core Yaxcopoil-1. In all localities, the spherule layers are in zone CF1, but only El Peñon and possibly Loma Cerca have the thick spherule unit suggesting primary deposition below the reworked spherules at the base of the sandstone complex. This impact spherule layer is near the base of zone CF1, although there is some erosion (undulating erosion surface, rip-up clasts). Zone CF1 spans the last 160 k.y. of the Maastrichtian below the K-T boundary (Fig. 3). A conservative estimate of spherule deposition is between 100 and 150 k.y. before the K-T boundary, which corresponds to the global warming (Li and Keller, 1998c; MacLeod et al., 2005; Abramovich et al., 2010; Keller et al., 2009d, 2011b; Punekar et al., this volume).

Probable age of reworked spherule layers. We can also estimate the depositional age of the reworked spherule layers at the base of the sandstone complex in the submarine channels, although this is more difficult because of downcutting and erosion. However, an age estimate can be made based on stable isotopes. Deposition occurred after the global warming, during a time of climate cooling and a sea-level fall in the upper half of zone CF1, as documented in the NE Mexico and Brazos River sections (Keller et al., 2007, 2009d, 2011b; Adatte et al., 1996, 2011; Punekar et al., this volume). This indicates that the sandstone complex (commonly called tsunami deposit) predates the K-T boundary by ~50–80 k.y. Near the end of the Maastrichtian, sea level rose again, and climate warmed across the K-T boundary, as observed in expanded sequences (e.g., El Kef and Elles, Tunisia, and Brazos River, Texas; Adatte et al., 2002, 2011; Abramovich et al., 2011; Keller et al., 2011b). No impact spherules are present at the K-T boundary in complete sequences (Keller et al., 2013).

Chicxulub and the K-T Boundary Mass Extinction

The stratigraphic position of the older impact spherule layers in undisturbed bedded marls and marly limestone at El Peñon and Loma Cerca permit evaluation of the environmental effects of the Chicxulub impact. Surprisingly, quantitative planktic foraminiferal analysis below and above the impact spherule layer at El Peñon reveals no significant change in species diversity or abundance, and all species survived with no long-term effects (Keller et al., 2009d). Similarly, no significant changes are observed in carbon isotopes or trace elements. The same results were earlier observed across the older impact spherule layers at Loma Cerca (Keller et al., 2002b). No mass extinction is associated with the spherules of the sandstone complex along the Brazos River, Texas, where the K-T boundary is up to 1.0 m up section (Keller et al., 2011b), or in the impact crater core Yaxcopoil-1, where the K-T boundary mass extinction is above a 0.5-m-thick limestone with five glauconitic clay horizons of zone CF1 age that overlies the impact breccia (Keller et al., 2004a, 2004b). These data suggest that the environmental effects of the Chicxulub impact were transient and not detectable within sample resolution of a few thousand years and that the kill effect of this impact has been overrated. Equally important is absence of impact spherules at the K-T boundary in complete sequences, which also indicates that this impact did not cause the mass extinction.

COINCIDENCE OF DECCAN VOLCANISM AND CHICXULUB IMPACT

Impact spherules are embedded in sediments at three different age intervals: (1) Most common are reworked spherule layers in the early Danian zone P1a, virtually always above a K-T boundary hiatus, as documented throughout the North Atlantic, Caribbean, and Central America (Fig. 14). (2) Impact spherules are restricted to the late Maastrichtian zone CF1 in over 80 sections of NE Mexico and Texas, where multiple spherule layers are reworked at the base of submarine channels (Figs. 14 and 15). (3) Also in NE Mexico (Loma Cerca and El Peñon), we find the stratigraphically oldest impact spherule layers in the late Maastrichtian near the base of zone CF1 (~100–150 k.y. prior to the K-T boundary), ~4–9 m below the submarine channels (Fig. 16). The late Maastrichtian has rarely been studied in NE Mexico, and a systematic investigation is likely to uncover more localities with the primary impact spherule deposits preserved similar to Loma Cerca and El Peñon.

We can now correlate the Chicxulub impact and Deccan volcanism, based on isotope stratigraphy and planktic foraminiferal biostratigraphy (Fig. 3). The onset of Deccan phase 2 volcanism began ~200 k.y. before the K-T boundary, coincident with rapid global warming that reached its maximum in the lower part of CF1. The stratigraphically oldest impact spherules near the base of zone CF1 occurred during this global warming. However, the 50 k.y. age uncertainty (between 100–150 k.y. prior to the K-T boundary) prevents evaluation of Chicxulub's contribution to the global warming. The impact may have exacerbated climate warming already under way due to Deccan volcanism, or it could have coincided with the onset of rapid global warming and resulted in intensified Deccan phase 2 volcanic eruptions.

The reworked spherules at the base of the sandstone complex with a depositional age of between 50 and 80 k.y. before the K-T boundary were deposited during global cooling and a sea-level fall. This appears to have been a time of decreased volcanic activity as suggested by geochemical data (Fig. 12; Keller et al., 2002b; Adatte et al., 1996). The single and multiple reworked impact spherule layers in early Danian sediments overlie a hiatus that juxtaposed Danian and late Maastrichtian zone CF3 (Keller et al., 2013). Erosion and redeposition occurred during a sea-level fall in the middle of zone P1a that has been documented in numerous deep-sea sections, including Haiti, Belize, Guatemala, and throughout the Caribbean (Keller et al., 1993, 2003a, 2003b, 2013). The fortuitous deposition of spherules overlying this hiatus (e.g., Bass River, New Jersey, ODP Sites 1049, 1259) is therefore not proof that the Chicxulub impact is precisely K-T boundary in age as frequently claimed.

REASSESSMENT OF THE MASS EXTINCTION SCENARIO

Over the past three decades, the hypothesis that a large extraterrestrial impact (Chicxulub) caused the mass extinction reached near-mythical status as the cause for the K-T boundary mass extinction and particularly the demise of the dinosaurs (Archibald, this volume). Evidence to the contrary was largely ignored or interpreted as the result of impact-induced giant earthquakes and tsunami waves creating massive gravity flows, slumps, margin collapse, faults, and folding that disturbed, mixed, or obliterated the sedimentary record. There is no doubt that a giant impact such as Chicxulub, creating a 175-km-diameter crater, would trigger tsunami and earthquakes, but are the resultant disturbed deposits preserved, and how are they identified?

Dypvik and Jansa (2003) observed that differentiating between gravity deposits triggered by rare impacts and those caused by common earthquakes is difficult and depends on the presence of melt-rock particles and iridium enrichments. For the Chicxulub impact, this is mainly the impact glass spherules surrounding the Chicxulub crater from the North Atlantic through the Caribbean and Central America (Fig. 14). However, Dypvik and Jansa (2003) observed a dearth of giant tsunami evidence associated with the Chicxulub impact outside the Gulf of Mexico, referring to the so-called tsunami deposits in the submarine channels of NE Mexico. As noted in this review, the sedimentary characteristics of these deposits demonstrate long-term deposition and repeated colonization of the seafloor that is incompatible with tsunami deposition.

In contrast to the popular Chicxulub impact hypothesis as cause for the K-T boundary mass extinction, Deccan volcanism—the other major catastrophe—has languished as an unlikely cause. However, over the past few years, researchers have made major advances in improved dating and correlation, identifying environmental changes based on basalt geochemistry and its weathering products, and based on micropaleontology documenting the direct link between the mass extinction and the massive flood basalt eruptions of phase 2 at the end of the Maastrichtian. Although much research remains to be done, the current data set for the first time permits evaluation of the age and faunal and environmental effects of Deccan volcanism in India and globally. Also for the first time, this database can be compared and correlated with the Chicxulub impact to evaluate the age, coincidence, and environmental effects of these two catastrophes. The following scenario integrates the major features of the Deccan and Chicxulub records in an effort to put the current data into context in order to better understand the events leading up to the K-T boundary mass extinction.

DECCAN VOLCANISM AND CHICXULUB IMPACT: AN INTEGRATED SCENARIO AND CONCLUSIONS

Deccan volcanism in palemagnetic chron C29r (planktic foraminiferal zones CF1–CF2) is linked to global climate and environmental changes ending with the K-T boundary mass extinction (Robinson et al., 2009; Keller et al., 2011a, 2012). Climate gradually cooled during the late Maastrichtian, reaching maximum cooling by the end of CF3, followed by rapid warming in the upper part of CF2 (Li and Keller, 1998c), beginning at ~200 k.y. before the K-T boundary (Fig. 17). Climate remained very warm but fluctuating until the middle of zone CF1, when it cooled and then warmed again near the end of the Maastrichtian (for high-resolution stable isotope records, see Punekar et al., this volume). Based on $^{187}Os/^{188}Os$ data, Robinson et al. (2009) speculated that a lower carbon burial rate during the last 200 k.y. of the Maastrichtian resulted from ocean acidification caused by Deccan volcanism. This age estimate is in agreement with the onset for Deccan phase 2 and warming in the upper part of zone CF2 but not with lower carbon burial, except near the end of the Maastrichtian (Font et al., 2011, this volume) (Fig. 3). Chenet et al. (2009) estimated that the entire phase 2 eruptions may have occurred within 100 k.y., with long periods of inactivity reducing active eruptions to possibly just 10 k.y. More precise age estimates must await better dating techniques, particularly the dating of single large eruptive events. Chenet et al. (2009) estimated the total gas output of Deccan phase 2 was up to 17,000 Gt of SO_2 and 35,000 Gt of CO_2, which is on the order of 20–200 times that of the Chicxulub impact (Courtillot and Fluteau, this volume).

The kill effect of volcanism depends not just on total gas output, but also on the rate of output and how fast eruptive events follow each other, preventing ecosystem recovery and causing runaway effects. The four largest lava flows of phase 2 near the end of the Maastrichtian followed each other in rapid succession and are separated by just 5 m, 10 m, and 15 m of sand and sandy shale, compared with marls in the infratrappean sediments of the Krishna-Godavari Basin wells (Fig. 10). This suggests a major change in sedimentation, with megaflow eruptions resulting in high clastic influx from the Krishna and Godavari Rivers over a short time span. If this was the case, then the rapid succession of massive volcanic eruptions at the end of phase 2 likely led to runaway effects, preventing ecosystem recovery and causing the mass extinction (Fig. 17).

Mass Extinction Crisis Onset: Stage 1

The crisis that led to the K-T boundary mass extinction began when Deccan volcanism reached critical levels during phase 2 in the latest Maastrichtian, depositing 80% of the entire

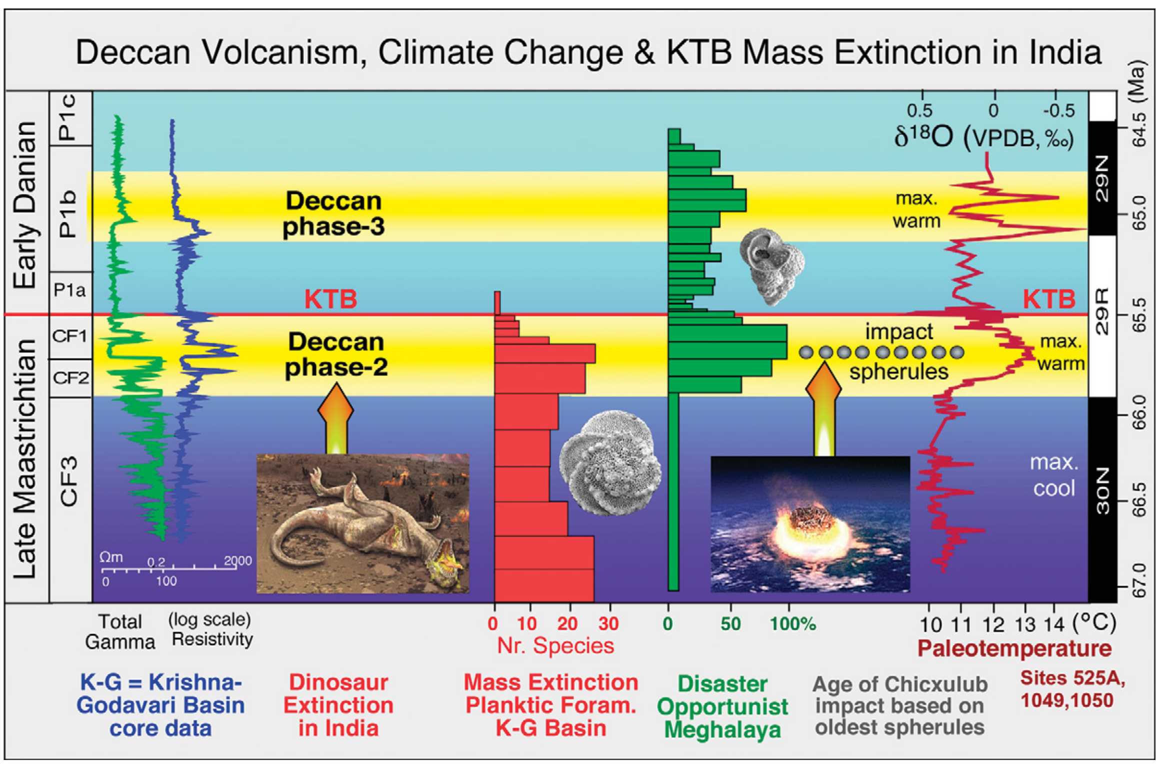

Figure 17. Summary of climatic, environmental, and biologic effects related to Deccan volcanism. All dinosaurs in India disappeared by the onset of the main eruptions in phase 2 (inset illustration at left: U.S. National Science Foundation, 2008); 50% of planktic foraminifera disappeared at this time, and nearly all went extinct by the fourth and last megaflow at the K-T boundary (KTB). Rapid climate changes and blooms of the disaster opportunist *Guembelitria cretacea* accompanied volcanic phase 2, in the early Danian after the mass extinction, and stress conditions intensified with eruptions of the last Deccan phase 3. The precise timing of the mass extinction is still uncertain. VPDB—Vienna Peedee belemnite.

3500-m-thick Deccan lava pile. With increasing volcanic intensity, SO_2 and CO_2 release led to acid rains on land and ocean acidification, which resulted in a carbonate crisis for marine organisms, as evident in dissolution effects and eventually extinctions (Robinson et al., 2009; Keller et al., 2011a, 2012; Font et al., 2011, this volume; Courtillot and Fluteau, this volume). The massive input of CO_2, beginning in the upper zone CF2 and continuing into the middle of CF1, led to the well-documented rapid global warming of 8 °C on land and 4 °C in the oceans worldwide (e.g., Li and Keller, 1998c; Wilf et al., 2003; Punekar et al., this volume).

During this global warming, high-stress marine environmental conditions resulted in the dominance (60%–80%) of the disaster opportunist *Guembelitria cretacea* worldwide, particularly in shallow-marine environments subjected to terrestrial, nutrient-rich, high runoff due to increased weathering (Fig. 13). On a global basis, the variable abundance of *Guembelitria* blooms and the decline in abundance of other species but no extinctions suggest that partial ecosystem recovery occurred between major volcanic eruptions, permitting species survival.

The Chicxulub impact on Yucatan occurred during this time, as indicated by the position of the stratigraphically oldest spherule layers in the lower part of CF1 in NE Mexico, Texas, and the pre–K-T boundary age of impact breccia in the crater. This impact likely contributed to and exacerbated the ongoing greenhouse warming and may have intensified volcanic eruptions. Environmental effects appear to have been short-term and transient, with no detectable changes in sample resolution of a few thousand years (Keller et al., 2004a, 2004b, 2009d, 2011b) (Fig. 17). No species extinctions are associated with this climate warming and impact. This indicates that the kill effect of the Chicxulub impact has been vastly overestimated.

Mass Extinction Crisis Middle: Stage 2

By the middle of zone CF1, greenhouse warming ended and climate cooled, accompanied by a falling sea level (Keller et al., 2007, 2011b). Intensified currents led to erosion, formation of submarine channels, and transport from nearshore areas into deeper waters, creating the sandstone complex known from submarine channels in NE Mexico and Texas and hiatuses elsewhere (Adatte et al., 1996). At this time, impact spherule deposits and shallow-water debris were repeatedly eroded from nearshore areas, transported seaward, and redeposited at the base of the sandstone complex. Subsequent sandstone deposition, with few spherule-filled burrows near the base, suggests gravity flows. The upper unit of fine sand, shale, and marl layers marks the rising sea level and return to normal sedimentation, with intensively burrowed horizons indicating colonization of the seafloor (Ekdale and Stinnesbeck, 1998). Popular scenarios interpret this sandstone complex as impact-generated tsunami deposits coeval with the K-T boundary and therefore place the mass extinction at the reworked impact spherule layers (e.g., Schulte et al., 2010).

Mass Extinction Crisis Ending: Stage 3

Near the end of the Maastrichtian, climate rapidly warmed, and sea level rose, eventually depositing the K-T boundary clay (Fig. 17). The largest four megaflow eruptions of the Krishna-Godavari Basin, spanning over 1500 km across India and out into the Bay of Bengal (Self et al., 2008), likely occurred during the last ~50 k.y. below the K-T boundary. This is suggested by (1) the maximum stress conditions below the K-T boundary in the Meghalaya section, where *Guembelitria* blooms reach 95%, ending with the mass extinction (Figs. 5 and 17; Gertsch et al., 2011a), (2) the Krishna-Godavari Basin wells where the onset of the mass extinction began just below the four megaflows, ending with the K-T boundary mass extinction (Figs. 10, 11, and 17), (3) the strong dissolution effects in intertrappean sediments (Figs. 5, 10, and 11; Keller et al., 2011a, 2012), and (4) strong dissolution effects in marine sections over an estimated ~30 k.y. below the K-T boundary mass extinction at Bidart, France (Font et al., 2011, this volume; Courtillot and Fluteau, this volume). Dissolution effects preceding the K-T boundary mass extinction have been observed by many paleontologists, but systematic documentation and evaluation on a global basis remain to be done.

Current data indicate that the mass extinction in planktic foraminifera occurred rapidly, beginning in infratrappean sediments just below the first of four megaflows, and was complete by the K-T boundary (Figs. 3, 10, 11, and 17). The last dinosaur remains are known from the infratrappean sediments below the megaflows, and their demise is interpreted as the direct result of Deccan volcanism (e.g., Samant and Mohabey, this volume; Prasad and Sahni, this volume). The immediate cause for the mass extinction was likely the rapid massive eruptions, increased volcanic intensity, and high SO_2 and CO_2 release, leading to runaway effects and preventing ecosystem recovery. The kill mechanism was likely arid climate and acid rains on land (Fig. 18), and ocean acidification in the marine realm, resulting in the observed carbonate crisis for marine organisms, as evident in dissolution effects and extinctions globally.

Environmental Effects in India

In the Deccan volcanic province, semiarid conditions known as "mock aridity" prevailed, whereas in the surrounding areas, abundant precipitation, acid rains, high chemical weathering, and continental runoff resulted in a major influx of silt and nutrients into the oceans (Fig. 12; Gertsch et al., 2011a). This led to increasingly toxic, turbid, mesotrophic to eutrophic waters, creating high-stress conditions that likely caused the mass extinction of nearly all planktic foraminifera. Enhanced weathering led to decreased CO_2 and pCO_2, reversing the global warming and leading to the rapid global cooling after the mass extinction. Parallel conditions have been observed associated with the Permian-Triassic volcanism and mass extinction. For example, Algeo and Twitchett (2010) reported high rates of physical and chemical erosion as a result of climate warming

Figure 18. Artist illustration of the end-Cretaceous mass extinction, including the dinosaur extinction, as a result of Deccan volcanism in India (U.S. National Science Foundation, 2008).

and acid rains at 16 Permian-Triassic mass extinction localities. They inferred that the resultant terrestrial ecosystem destruction, erosion, and runoff led to marine siltation and eutrophication, which contributed to the marine biotic crisis and delayed recovery after the mass extinction.

Mass Extinction After Effects: Stage 4

A few tiny, stress-tolerant planktic foraminiferal species evolved very quickly after the mass extinction. During the early Danian zone P1a (C29R), environmental stress conditions remained high, possibly because of continued high nutrient influx from weathering, as evident in the high total organic content of sediments (Gertsch et al., 2011a). As a result, marine productivity recovered only minimally, as evident by the very low species diversity, increasing from 5 to 12 species over ~300 k.y. (Figs. 5 and 10). All evolving species remained very small (<100 µm, frequently <63 µm), unornamented, and simple in morphology, reflecting the continued high-stress conditions. *Guembelitria* blooms prevailed, but generally of lower abundance compared with the latest Maastrichtian, and decreased shortly after the K-T boundary in India and globally (Figs. 13; Punekar et al., this volume). However, preservation of carbonate shells is very good, indicating no significant dissolution effects and absence of ocean acidification. This indicates that volcanic activity was largely absent in the early Danian (C29R, zone P1a) and that continued weathering of basalts resulted in the increased nutrient input and high-stress marine environment that delayed biotic recovery.

Early Danian Crisis—Deccan Volcanism Phase 3

The last Deccan phase 3 began at the base of C29N (zone P1b) accompanied by the extinction of *Parvularugoglobigerina eugubina* and *P. longiapertura* and decreased abundances of other earliest Danian species. No significant extinctions occurred during phase 3 volcanism, probably because eruptions were widely separated in time, permitting ecosystem recovery. Alternatively, the small early Danian species that evolved in the aftermath of the mass extinction were more stress tolerant than the specialized large Maastrichtian species and therefore able to survive the stress conditions associated with the Deccan phase 3. In contrast to the latest Maastrichtian, dissolution effects are minor, suggesting no significant change in marine pH conditions. However, species diversity remained low (<15 species), and simple, small morphotypes prevailed similar to zone P1a.

A gradual recovery to larger morphotypes and higher diversity began only after the Deccan phase 3 ended, and full recovery was restored with normal nutrient input and the return to oligotrophic conditions. This suggests that the long-delayed post–K-T boundary marine recovery that has remained an enigma for decades (e.g., Keller and Benjamini, 1991; Magaritz et al., 1992) was due to continued high-stress conditions induced by Deccan volcanism and its weathering products. Punekar et al. (this volume) detail the faunal event associated with Deccan phase 3 and its environmental and climatic consequences.

CONCLUSIONS

The proposed scenario for the K-T boundary mass extinction and delayed recovery is based on integration of large, multidisciplinary data sets on Deccan volcanism, the Chicxulub impact, and the mass extinction. It takes into consideration climate warming and cooling, sea-level changes, erosion, weathering, ocean acidification, high-stress environments with opportunistic species blooms, the mass extinction, and delayed postextinction recovery. The scenario based on all of these factors is necessarily complex, and no single event, such as the Chicxulub impact, can account for the observed long-term environmental and biotic changes. The Chicxulub impact coincided with the major late Maastrichtian rapid warming of 4 °C in the oceans and 8 °C on land that is commonly attributed to Deccan volcanism, and it may have significantly contributed to this warming and even intensified volcanic eruptions. This rapid warming triggered the observed cascade of climate changes and high environmental stress conditions that eventually led to the K-T boundary mass extinction and delayed recovery. Near the end of the Maastrichtian, another series of at least four massive volcanic eruptions in short order formed the longest lava flows on Earth and probably caused runaway effects, particularly ocean acidification, which resulted in the carbonate crisis commonly considered to be the prime cause for the mass extinction. The Chicxulub impact played no role in this mass extinction. The post–K-T boundary high-stress conditions and delayed recovery can be attributed to weathering of volcanic rocks followed by the last phase 3 of Deccan volcanism, delaying recovery.

ACKNOWLEDGMENTS

The review comments and suggestions of Richard Twitchett and Bill MacDonald are greatly appreciated and clarified various issues. The work presented in this review is the result of over two decades working on K-T boundary sequences with Chicxulub impact ejecta and 6 yr on Deccan volcanism, most of it in collaboration with Thierry Adatte and many other collaborators, as well as former and current students. Over the past 5 yr, many Indian colleagues have contributed to Deccan studies and field-based research, including Sunil Bajpai, Dhananjay Mohabey, Bandana Samant, Rahul Garg, and Nallamuthu Malarkodi. Research on deep wells in the Krishna-Godavari Basin would not have been possible without the permission and support of former directors D.K. Pande and S.V. Rao of the Oil and Natural Gas Corporation of India, the facilitation of Harinder Upadhyay, and the collaboration of its scientists, particularly B.C. Jaiprakash, A.N. Reddy, and D.S.N. Raju. This study is based upon work supported by the U.S. National Science Foundation (NSF) through the Continental Dynamics Program, Sedimentary Geology, and Paleobiology Program, and Office of International Science and Engineering's India Program under NSF grants EAR-0207407, EAR-0447171, and EAR-1026271.

REFERENCES CITED

Abramovich, S., and Keller, G., 2002, High stress late Maastrichtian paleoenvironment: Inference from planktonic foraminifera in Tunisia: Palaeogeography, Palaeoclimatology, Palaeoecology, v. 178, p. 145–164, doi:10.1016/S0031-0182(01)00394-7.

Abramovich, S., Almogi-Labin, A., and Benjamini, Ch., 1998, Decline of the Maastrichtian pelagic ecosystem based on planktic foraminifera assemblage changes: Implication for the terminal Cretaceous faunal crisis: Geology, v. 26, p. 63–66.

Abramovich, S., Yovel-Corem, S., Almogi-Labin, A., and Benjamini, C., 2010, Global climate change and planktic foraminiferal response in the Maastrichtian: Paleoceanography, v. 25, PA2201, doi:10.1029/2009PA001843.

Abramovich, S., Keller, G., Berner, Z., Cymbalista, M., and Rak, C., 2011, Maastrichtian planktic foraminiferal biostratigraphy and paleoenvironment of Brazos River, Falls County, Texas, *in* Keller, G., and Adatte, T., eds., The End-Cretaceous Mass Extinction and the Chicxulub Impact in Texas: Society for Sedimentary Geology (SEPM) Special Publication 100, p. 123–156.

Adatte, T., Stinnesbeck, W., and Keller, G., 1996, Lithostratigraphic and mineralogical correlations of near-K/T boundary clastic sediments in NE Mexico: Implications for origin and nature of deposition, *in* Ryder, G., Fastovsky, D., and Gartner, S., eds., The Cretaceous-Tertiary Event and Other Catastrophes in Earth History: Geological Society of America Special Paper 307, p. 211–226.

Adatte, T., Keller, G., Burns, S., Stoykova, K.H., Ivanov, M.I., Vangelov, D., Kramar, U., and Stüben, D., 2002, Paleoenvironment across the Cretaceous-Tertiary transition in eastern Bulgaria, *in* Koeberl, C., and MacLeod, K.G., eds., Catastrophic Events and Mass Extinctions: Impacts and Beyond: Geological Society of America Special Paper 356, p. 231–252.

Adatte, T., Keller, G., and Baum, G., 2011, Lithostratigraphy, sedimentology, sequence stratigraphy and the origin of the sandstone complex in the Brazos River KT sequences, *in* Keller, G., and Adatte, T., eds., The End-Cretaceous Mass Extinction and the Chicxulub Impact in Texas: Society for Sedimentary Geology (SEPM) Special Publication 100, p. 43–80.

Alegret, L., Molina, E., and Thomas, E., 2001, Benthic foraminifera at the Cretaceous-Tertiary boundary around the Gulf of Mexico: Geology, v. 29, no. 10, p. 891–894, doi:10.1130/0091-7613(2001)029<0891:BFATCT>2.0.CO;2.

Algeo, T.J., and Twitchett, R.J., 2010, Anomalous Early Triassic sediment fluxes due to elevated weathering rates and their biological consequences: Geology, v. 38, p. 1023–1026, doi:10.1130/G31203.1.

Archibald, D.J., 2014, this volume, What the dinosaur record says about extinction scenarios, *in* Keller, G., and Kerr, A.C., eds., Volcanism, Impacts, and Mass Extinctions: Causes and Effects: Geological Society of America Special Paper 505, doi:10.1130/2014.2505(10).

Archibald, D.J., Archibald, J.D., Clemens, W.A., Padian, K., Rowe, T., MacLeod, N., Barrett, P.M., Gale, A.S., Holroyd, P., Sues, H.-D., Arens, N.C., Horner, J.R., Wilson, G.P., Goodwin, M.B., Brochu, C.A., Lofgren, D.L., Hurlbert, S.H., Hartman, J.A., Eberth, D.A., Wignall, P.B., Currie, P.J., Weil, A., Prasad, G.V.R., Dingus, L., Courtillot, V., Milner, A., Milner, A., Bajpai, S., Ward, D.J., and Sahni, A., 2010, Cretaceous extinctions: Multiple causes: Science, v. 328, p. 973.

Arenillas, I., Arz, J.A., Grajales-Nishimura, J.M., Murillo-Muneton, G., Alvarez, W., Camargo-Zanguera, A., Molina, E., and Rosales-Dominguez, C., 2006, Chicxulub impact event is Cretaceous/Paleogene boundary in age: New micropaleontological evidence: Earth and Planetary Science Letters, v. 249, p. 241–257, doi:10.1016/j.epsl.2006.07.020.

Arz, J.A., Alegret, L., and Arenillas, I., 2004, Foraminiferal biostratigraphy and environmental reconstruction at the Yaxcopoil-1 drillcore, Chicxulub crater, Yucatan Peninsula: Meteoritics & Planetary Science, v. 39, no. 7, p. 1099–1111, doi:10.1111/j.1945-5100.2004.tb01131.x.

Badve, R.M., and Ghare, M.A., 1977, Palaeoecological aspects of the Bagh Beds, India: Recent Researches in Geology, v. 4, p. 388–402.

Bajpai, S., and Prasad, G.V.R., 2000, Cretaceous age for Ir-rich Deccan intertrappean deposits: Palaeontological evidence from Anjar, western India: Journal of the Geological Society of London, v. 157, p. 257–260, doi:10.1144/jgs.157.2.257.

Bajpai, S., Holmes, J., Bennett, C., Mandal, N., and Khosla, A., 2013, Paleoenvironment of northwestern India during the Late Cretaceous Deccan volcanic episode from trace element and stable isotope geochemistry of intertrappean ostracod shells: Global and Planetary Change, v. 107, p. 82–90, doi:10.1016/j.gloplacha.2013.04.011.

Baksi, A.K., 2005, Comment on "^{40}Ar/^{39}Ar dating of the Rajahmundry Traps, eastern India and their relations to the Deccan Traps" by Knight et al.: Earth and Planetary Science Letters, v. 239, p. 368–373, doi:10.1016/j.epsl.2005.03.029.

Baksi, A.K., Byerly, G.R., Chan, L.-H., and Farrar, E., 1994, Intracanyon flows in the Deccan province, India: Case history of the Rajahmundry Traps: Geology, v. 22, p. 605–608, doi:10.1130/0091-7613(1994)022<0605:IFITDP>2.3.CO;2.

Berggren, W.A., Kent, D.V., Swisher, C.C., III, and Aubry, M.-P., 1995, A revised Cenozoic geochronology and chronostratigraphy, *in* Berggren, W.A., Kent, D.V., Aubry, M.-P., and HardenboL, J., eds., Geochronology, Time Scales and Global Stratigraphic Correlation: Society for Sedimentary Geology (SEPM) Special Publication 54, p. 129–212.

Bhandari, A., 1995, Ostracodes from the inter-trappean beds near Duddukuru, Andhra Pradesh, and a note on their age and paleoecological significance: Indian Journal Petroleum Geology, v. 4, no. 1, p. 89–107.

Bhandari, N., Shukla, P.N., and Castognoli, C.G., 1993, Geochemistry of some K/T sections in India: Palaeogeography, Palaeoclimatology, Palaeoecology, v. 104, p. 199–211, doi:10.1016/0031-0182(93)90131-2.

Bhandari, N., Gupta, M., Panday, J., and Shukla, P.N., 1994, Chemical profiles in K/T boundary section of Meghalaya, India: Cometary, asteroidal or volcanic: Chemical Geology, v. 113, p. 45–60, doi:10.1016/0009-2541(94)90004-3.

Bhandari, N., Shukla, P.N., Ghevariya, Z.G., and Sundaram, S.M., 1996, K/T boundary layer in Deccan intertrappeans at Anjar, Kutch, *in* Ryder, G., Fastovsky, D., and Gartner, S., eds., The Cretaceous-Tertiary Event and Other Catastrophes in Earth History: Geological Society of America Special Paper 307, p. 417–424.

Blackburn, T.J., Olsen, P.E., Bowring, S.A., McLean, M.N., Kent, D.V., Puffer, J., McHone, G., Rasbury, T.E., and Et-Touhami, N.M., 2013, Zircon U-Pb geochronology links the end-Triassic extinction with the Central Atlantic magmatic province: Science, v. 340, p. 941–945, doi:10.1126/science.1234204.

Bodas, M.S., Khadri, S.F.R., and Subbarao, K.V., 1988, Stratigraphy of the Jawhar and Igatpuri Formations, Western Ghats Lava Pile, India, *in* Subbarao, K.B., ed., Deccan Flood Basalt: Geological Society of India Memoir 10, p. 235–252.

Bond, D.P.G., and Wignall, P.B., 2014, this volume, Large igneous provinces and mass extinctions: An update, *in* Keller, G., and Kerr, A.C., eds., Volcanism, Impacts, and Mass Extinctions: Causes and Effects: Geological Society of America Special Paper 505, doi:10.1130/2014.2505(02).

Bourgeois, J., Hansen, T.A., Wiberg, P.L., and Kauffman, E.G., 1988, A tsunami deposit at the Cretaceous-Tertiary boundary in Texas: Science, v. 241, p. 567–570, doi:10.1126/science.241.4865.567.

Chatterjee, S., Guven, N., Yoshenobu, A., and Donofrio, R., 2006, Shiva Structure: A Possible KT Boundary Impact Crater on the Western Shelf of India: Special Publications, Museum Texas Tech University, v. 50, 39 p.

Chenet, A.-L., Quidelleur, X., Fluteau, F., Courtillot, V., and Bajpai, S., 2007, ^{40}K/^{40}Ar dating of the main Deccan large igneous province: Further evidence of KTB age and short duration: Earth and Planetary Science Letters, v. 263, p. 1–15, doi:10.1016/j.epsl.2007.07.011.

Chenet, A.-L., Fluteau, F., Courtillot, V., Gerard, M., and Subbarao, K.V., 2008, Determination of rapid Deccan eruptions across the Cretaceous-Tertiary boundary using paleomagnetic secular variation: Results from a 1200-m-thick section in the Mahabaleshwar: Journal of Geophysical Research, v. 113, B04101, doi:10.1029/2006JB004635.

Chenet, A.-L., Courtillot, V., Fluteau, F., Gerard, M., Quidelleur, X., Khadri, S.F.R., Subbarao, K.V., and Thordarson, T., 2009, Determination of rapid Deccan eruptions across the Cretaceous-Tertiary boundary using paleomagnetic secular variation: 2. Constraints from analysis of eight new sections and synthesis for a 3500-m-thick composite section: Journal of Geophysical Research, v. 114, B06103, doi:10.1029/2008JB005644.

Coccioni, R., and Luciani, V., 2006, *Guembelitria irregularis* bloom at the K-T boundary: Morphological abnormalities induced by impact-related extreme environmental stress?, *in* Cockell, C., Koeberl, C., and Gilmour, I., eds., Biological Processes Associated with Impact Events: Impact Studies: Berlin, Springer, p. 179–196.

Colodner, D.C., Boyle, E.A., Edmond, J.M., and Thomson, J., 1992, Post-depositional mobility of platinum, iridium, and rhenium in marine sediments: Nature, v. 358, p. 402–404, doi:10.1038/358402a0.

Courtillot, V., and Fluteau, F., 2010, Cretaceous extinctions: The volcanic hypothesis: Science, v. 328, p. 973–974, doi:10.1126/science.328.5981.973-b.

Courtillot, V., and Fluteau, F., 2014, this volume, A review of the embedded time scales of flood basalt volcanism with special emphasis on dramatically short magmatic pulses, *in* Keller, G., and Kerr, A.C., eds., Volcanism, Impacts, and Mass Extinctions: Causes and Effects: Geological Society of America Special Paper 505, doi:10.1130/2014.2505(15).

Courtillot, V., and Renne, J., 2003, On the ages of flood basalt events: Comptes Rendus Geoscience, v. 335, p. 113–140, doi:10.1016/S1631-0713(03)00006-3.

Courtillot, V., Besse, J., Vandamme, D., Montigny, R., Jaeger, J.-J., and Cappetta, H., 1986, Deccan flood basalts at the Cretaceous/Tertiary boundary?: Earth and Planetary Science Letters, v. 80, p. 361–374, doi:10.1016/0012-821X(86)90118-4.

Courtillot, V., Feraud, G., Maluski, H., Vandamme, D., Moreau, M.G., and Besse, J., 1988, The Deccan flood basalts and the Cretaceous-Tertiary boundary: Nature, v. 333, p. 843–846, doi:10.1038/333843a0.

Courtillot, V., Gallet, Y., Rocchia, R., Feraud, G., Robin, E., Hofmann, C., Bhandari, N., and Ghevariya, Z.G., 2000, Cosmic markers, ^{40}Ar/^{39}Ar dating and paleomagnetism of the KT sections in the Anjar area of the Deccan large igneous province: Earth and Planetary Science Letters, v. 182, p. 137–156, doi:10.1016/S0012-821X(00)00238-7.

Cowie, J.W., Ziegler, W., and Remane, J., 1989, Stratigraphic Commission accelerates progress, 1984 to 1989: Episodes, v. 12, p. 79–83.

Crocket, J.H., and Paul, D.K., 2004, Platinum-group elements in Deccan mafic rocks: A comparison of suites differentiated by Ir contents: Chemical Geology, v. 208, p. 273–291, doi:10.1016/j.chemgeo.2004.04.017.

Dessert, C., Dupre, B., Gaillardet, J., Francois, L.M., and Allegre, C.J., 2003, Basalt weathering laws and the impact of basalt weathering on the global carbon cycle: Chemical Geology, v. 202, p. 257–273, doi:10.1016/j.chemgeo.2002.10.001.

Dypvik, H., and Jansa, L.F., 2003, Sedimentary signatures and processes during marine bolide impacts: A review: Sedimentary Geology, v. 161, p. 309–337, doi:10.1016/S0037-0738(03)00135-0.

Ekdale, A.A., and Stinnesbeck, W., 1998, Ichnology of Cretaceous-Tertiary (K/T) boundary beds in northeastern Mexico: Palaios, v. 13, p. 593–602, doi:10.2307/3515350.

Font, E., Nedelec, A., Ellwood, B.B., Mirao, J., and Silva, P.F., 2011, A new sedimentary benchmark for the Deccan Traps volcanism?: Geophysical Research Letters, v. 38, p. L24309, doi:10.1029/2011GL049824.

Font, E., Fabre, S., Nédélec, A., Adatte, T., Keller, G., Veiga-Pires, C., Ponte, J., Mirão, J., Khozyem, H., and Spangenberg, J., 2014, this volume, Atmospheric halogen and acid rains during the main phase of Deccan eruptions: Magnetic and mineral evidence, *in* Keller, G., and Kerr, A.C., eds., Volcanism, Impacts, and Mass Extinctions: Causes and Effects: Geological Society of America Special Paper 505, doi:10.1130/2014.2505(18).

Gale, A., 2006, The Cretaceous-Tertiary boundary on the Brazos River, Falls County, Texas; evidence for impact-induced tsunami sedimentation?: Proceedings of the Geologists' Association, v. 117, p. 1–13.

Garg, R., Khowaja-Ateequzzaman, and Prasad, V., 2006, Significant dinoflagellate cyst biohorizons in the Upper Cretaceous–Palaeocene succession of the Khasi Hills, Meghalaya: Journal Geological Society of India, v. 67, p. 737–747.

Gertsch, B., Keller, G., Adatte, T., Garg, R., Prasad, V., Fleitmann, D., and Berner, Z., 2011a, Environmental effects of Deccan volcanism across the Cretaceous-Tertiary transition in Meghalaya, India: Earth and Planetary Science Letters, v. 310, p. 272–285.

Gertsch, B., Keller, G., Adatte, T., and Berner, Z., 2011b, Platinum group element (PGE) geochemistry of Brazos sections, Texas, *in* Keller, G., and Adatte, T., eds., End-Cretaceous Mass Extinction and the Chicxulub Impact in Texas: Society for Sedimentary Geology (SEPM) Special Publication 100, p. 228–249.

Govindan, A., 1981, Foraminifera from the infra- and intertrappean subsurface sediments of Narsapur Well-1 and age of the Deccan Trap flows, *in* Khosla, S.C., and Kachara, R.P., eds, Proceedings of the 9th Indian Colloquium of Micropalaeontology and Stratigraphy, p. 81–93.

Gradstein, F., Ogg, J., and Smith, A., 2004, A Geologic Time Scale: Cambridge, UK, Cambridge University Press, 598 p.

Harris, J., and Van Couvering, J., 1995, Mock aridity and the paleoecology of volcanically influenced ecosystems: Geology, v. 23, p. 593–596, doi:10.1130/0091-7613(1995)023<0593:MAATPO>2.3.CO;2.

Hart, M.B., Searle, S., Feist, S.E., Leighton, A.D., Price, G.D., Smart, C.W., and Twitchett, R.J., 2011, The distribution of benthic foraminifera across the Cretaceous-Paleogene boundary in Texas (Brazos River) and Denmark (Stevns Klint), *in* Keller, G., and Adatte, T., eds., The End-Cretaceous Mass Extinction and the Chicxulub Impact in Texas: Society for Sedimentary Geology (SEPM) Special Publication 100, p. 179–196.

Hart, M.B., Yancey, T.E., Leighton, A.D., Miller, B., Liu, C., Smart, C.W., and Twitchett, R.J., 2012, The Cretaceous-Paleogene boundary on the Brazos River, Texas: New stratigraphic sections and revised interpretations: Gulf Coast Association of Geological Societies Journal, v. 1, p. 69–80.

Heymann, D., Yancey, T.E., Wolbach, W.S., Thiemens, M.H., Johnson, E.A., Roach, D., and Moecker, S., 1998, Geochemical markers of the Cretaceous-Tertiary boundary event at Brazos River, Texas, USA: Geochimica et Cosmochimica Acta, v. 62, no. 1, p. 173–181, doi:10.1016/S0016-7037(97)00330-X.

Hofmann, C., Feraud, G., and Courtillot, V., 2000, 40Ar/39Ar dating of mineral separates and whole rocks from the Western Ghats lava pile: Further constraints on duration and age of the Deccan Traps: Earth and Planetary Science Letters, v. 180, p. 13–27, doi:10.1016/S0012-821X(00)00159-X.

Jaiprakash, B.C., Singh, J., and Raju, D.S.N., 1993, Foraminiferal events across the K/T boundary and age of Deccan volcanism in Palakollu area, Krishna-Godavari Basin, India: Journal of the Geological Society of India, v. 41, p. 105–117.

Jay, A.E., and Widdowson, M., 2008, Stratigraphy, structure and volcanology of the south-east Deccan continental flood basalt province: Implications for eruptive extent and volumes: Journal of the Geological Society of London, v. 165, p. 177–188, doi:10.1144/0016-76492006-062.

Jay, A.E., MacNiocaill, C., Widdowson, M., Self, S., and Turner, W., 2009, New palaeomagnetic data from the Mahabaleshwar Plateau, Deccan flood basalt province, India: Implications for the volcanostratigraphic architecture of continental flood basalt provinces: Journal of the Geological Society of London, v. 166, p. 13–24, doi:10.1144/0016-76492007-150.

Keller, G., 2008, Impact Stratigraphy: Old principle, new reality, *in* Evans, K.R., Horton, J.W., and King, D.T., eds., The Sedimentary Record of Meteorite Impacts: Geological Society of America Special Paper 437, p. 147–178.

Keller, G., 2011, Defining the Cretaceous-Tertiary boundary: A practical guide and return to first principles, *in* Keller, G., and Adatte, T., eds., The End-Cretaceous Mass Extinction and the Chicxulub Impact in Texas: Society for Sedimentary Geology (SEPM) Special Publication 100, p. 23–42.

Keller, G., and Abramovich, S., 2009, Lilliput effect in late Maastrichtian planktic foraminifera: Response to environmental stress: Palaeogeography, Palaeoclimatology, Palaeoecology, v. 284, p. 47–62, doi:10.1016/j.palaeo.2009.08.029.

Keller, G., and Benjamini, C., 1991, Paleoenvironment of the eastern Tethys in the early Danian: Palaios, v. 6, p. 439–464, doi:10.2307/3514984.

Keller, G., and Pardo, A., 2004, Disaster opportunists Guembelitrinidae—Index for environmental catastrophes: Marine Micropaleontology, v. 53, p. 83–116, doi:10.1016/j.marmicro.2004.04.012.

Keller, G., Lyons, J.B., MacLeod, N., and Officer, C.B., 1993, Is there evidence for Cretaceous-Tertiary boundary impact deposits in the Caribbean and Gulf of Mexico?: Geology, v. 21, p. 776–780, doi:10.1130/0091-7613(1993)021<0776:ITEFCT>2.3.CO;2.

Keller, G., Li, L., and Macleod, N., 1995, The Cretaceous/Tertiary boundary stratotype section at El Kef, Tunisia: How catastrophic was the mass extinction?: Palaeogeography, Palaeoclimatology, Palaeoecology, v. 119, p. 221–254, doi:10.1016/0031-0182(95)00009-7.

Keller, G., Lopez-Oliva, J.G., Stinnesbeck, W., and Adatte, T., 1997, Age, stratigraphy and deposition of near-K/T siliciclastic deposits in Mexico: Relation to bolide impact?: Geological Society of America Bulletin, v. 109, p. 410–428, doi:10.1130/0016-7606(1997)109<0410:ASADON>2.3.CO;2.

Keller, G., Adatte, T., Stinnesbeck, W., Luciani, V., Karoui, N., and Zaghbib-Turki, D., 2002a, Paleoecology of the Cretaceous-Tertiary mass extinction in planktic foraminifera: Palaeogeography, Palaeoclimatology, Palaeoecology, v. 178, p. 257–297, doi:10.1016/S0031-0182(01)00399-6.

Keller, G., Adatte, T., Stinnesbeck, W., Affolter, M., Schilli, L., and Lopez-Oliva, J.G., 2002b, Multiple spherule layers in the late Maastrichtian of northeastern Mexico, *in* Koeberl, C., and MacLeod, K.G., eds., Catastrophic Events and Mass Extinctions: Geological Society of America Special Paper 356, p. 145–162.

Keller, G., Stinnesbeck, W., Adatte, T. and Stueben, D., 2003a, Multiple impacts across the Cretaceous-Tertiary boundary: Earth-Science Reviews, v. 62, p. 327–363.

Keller, G., Stinnesbeck, W., Adatte, T., Holland, B., Stueben, D., Harting, M., de Leon, C., and de la Cruz, J., 2003b, Spherule deposits in Cretaceous-Tertiary boundary sediments in Belize and Guatemala: Journal of the Geological Society of London, v. 160, p. 783–795, doi:10.1144/0016-764902-119.

Keller, G., Adatte, T., Stinnesbeck, W., Rebolledo-Vieyra, M., Urrutia Fucugauchi, J., Kramar, G., and Stueben, D., 2004a, Chicxulub predates the K/T boundary mass extinction: Proceedings of the National Academy of Sciences of the United States of America, v. 101, p. 3753–3758, doi:10.1073/pnas.0400396101.

Keller, G., Adatte, T., and Stinnesbeck, W., 2004b, More evidence that Chicxulub predates KT boundary: Meteoritics & Planetary Science, v. 39, no. 6/7, p. 1127–1144, doi:10.1111/j.1945-5100.2004.tb01133.x.

Keller, G., Adatte, T., Berner, Z., Harting, M., Baum, G., Prauss, M., Tantawy, A.A., and Stüben, D., 2007, Chicxulub impact predates KT boundary: New evidence from Brazos, Texas: Earth and Planetary Science Letters, v. 255, no. 3–4, p. 339–356, doi:10.1016/j.epsl.2006.12.026.

Keller, G., Adatte, T., Gardin, S., Bartolini, A., and Bajpai, S., 2008, Main Deccan volcanism phase ends near the K-T boundary: Evidence from the Krishna-Godavari Basin, SE India: Earth and Planetary Science Letters, v. 268, p. 293–311, doi:10.1016/j.epsl.2008.01.015.

Keller, G., Adatte, T., Bajpai, S., Mohabey, D.M., Widdowson, M., Khosla, A., Sharma, R., Khosla, S.C., Gertsch, B., Fleitmann, D., and Sahni, A., 2009a, K-T transition in Deccan Traps and intertrappean beds in central India mark major marine seaway across India: Earth and Planetary Science Letters, v. 282, p. 10–23, doi:10.1016/j.epsl.2009.02.016.

Keller, G., Khosla, S.C., Sharma, R., Khosla, A., Bajpai, S., and Adatte, T., 2009b, Early Danian planktic foraminifera from Cretaceous-Tertiary intertrappean beds at Jhilmili, Chhindwara District, Madhya Pradesh, India: Journal of Foraminiferal Research, v. 39, no. 1, p. 40–55, doi:10.2113/gsjfr.39.1.40.

Keller, G., Sahni, A., and Bajpai, S., 2009c, Deccan volcanism, the KT mass extinction and dinosaurs: Journal of Biosciences, v. 34, p. 709–728, doi:10.1007/s12038-009-0059-6.

Keller, G., Adatte, T., Pardo Juez, A., and Lopez-Oliva, J., 2009d, New evidence concerning the age and biotic effects of the Chicxulub impact in NE Mexico: Journal of the Geological Society of London, v. 166, p. 393–411, doi:10.1144/0016-76492008-116.

Keller, G., Adatte, T., Pardo, A., Bajpai, S., Khosla, A., and Samant, B., 2010, Cretaceous extinctions: Evidence overlooked: Science, v. 328, p. 974–975, doi:10.1126/science.328.5981.974-a.

Keller, G., Bhowmick, P.K., Upadhyay, H., Dave, A., Reddy, A.N., Jaiprakash, B.C., and Adatte, T., 2011a, Deccan volcanism linked to the Cretaceous-Tertiary boundary (KTB) mass extinction: New evidence from ONGC wells in the Krishna-Godavari Basin, India: Journal of the Geological Society of India, v. 78, p. 399–428, doi:10.1007/s12594-011-0107-3.

Keller, G., Abramovich, S., Adatte, T., and Berner, Z., 2011b, Biostratigraphy, age of the Chicxulub impact, and depositional environment of the Brazos River KTB sequences, *in* Keller, G., and Adatte, T., eds., The End-Cretaceous Mass Extinction and the Chicxulub Impact in Texas: Society for Sedimentary Geology (SEPM) Special Publication 100, p. 81–122.

Keller, G., Adatte, T., Bhowmick, P.K., Upadhyay, H., Dave, A., Reddy, A.N., and Jaiprakash, B.C., 2012, Nature and timing of extinctions in Cretaceous-Tertiary planktic foraminifera preserved in Deccan intertrappean sediments of the Krishna-Godavari Basin, India: Earth and Planetary Science Letters, v. 341–344, p. 211–221, doi:10.1016/j.epsl.2012.06.021.

Keller, G., Malarkodi, N., Khozeym, H., Adatte, T., Spangenberg, J.E., and Stinnesbeck, W., 2013, Chicxulub impact spherules in the NW Atlantic and Caribbean: Age constraints and KTB hiatus: Geological Magazine, v. 150, no. 5, p. 885–907, doi:10.1017/S0016756812001069.

Khadkikar, A.S., Sant, D.A., Gogte, V., and Karanth, R.V., 1999, The influence of Deccan volcanism in climate: Insights from lacustrine intertrappean deposits, Anjar, western India: Palaeogeography, Palaeoclimatology, Palaeoecology, v. 147, p. 141–149, doi:10.1016/S0031-0182(98)00156-4.

Khadri, S.F.R., Subbarao, K.V., Hooper, P.R., and Walsh, J.N., 1988, Stratigraphy of Thakurvadi Formation, western Deccan basalt province, India, *in* Subbarao, K.B., ed., Deccan Flood Basalt: Geological Society of India Memoir 10, p. 281–304.

Khosla, S.C., and Nagori, M.L., 2002, Ostracodes from the intertrappean beds (early Paleocene) of the east coast of India: Palaeontological Research, v. 6, no. 2, p. 191–210.

Khosla, S.C., Nagori, M.L., Jakhar, S.R., and Rathore, A.S., 2009, Mixed marine brackish water and non-marine microfaunal association in the intertrappean beds (early Paleocene) of Jhilmili, Chhindwara District, Madhya Pradesh: Journal of the Geological Society of India, v. 73, p. 724–732, doi:10.1007/s12594-009-0056-2.

Knight, K.B., Renne, P.R., Halkett, A., and White, N., 2003, $^{40}Ar/^{39}Ar$ dating of the Rajahmundry Traps, eastern India, and their relationship to the Deccan Traps: Earth and Planetary Science Letters, v. 208, p. 85–99, doi:10.1016/S0012-821X(02)01154-8.

Knight, K.B., Renne, P.R., Baker, J., Waight, T., and White, N., 2005, Reply to "$^{40}Ar/^{39}Ar$ dating of the Rajahmundry Traps, eastern India, and their relationship to the Deccan Traps: Discussion" by A.K. Baksi: Earth and Planetary Science Letters, v. 239, p. 374–382, doi:10.1016/j.epsl.2005.08.013.

Kuiper, K.F., Deino, A., Hilgen, F.J., Krijgsman, W., Renne, P.R., and Wijbrans, J.R., 2008, Synchronizing rock clocks of Earth history: Science, v. 320, p. 500–504, doi:10.1126/science.1154339.

Li, L., and Keller, G., 1998a, Maastrichtian climate, productivity and faunal turnovers in planktic foraminifera of South Atlantic DSDP Sites 525A and 21: Marine Micropaleontology, v. 33, no. 1–2, p. 55–86, doi:10.1016/S0377-8398(97)00027-3.

Li, L., and Keller, G., 1998b, Diversification and extinction in Campanian-Maastrichtian planktic foraminifera of northwestern Tunisia: Eclogae Geologica Helvetiae, v. 91, p. 75–102.

Li, L., and Keller, G., 1998c, Abrupt deep-sea warming at the end of the Cretaceous: Geology, v. 26, p. 995–998, doi:10.1130/0091-7613(1998)026<0995:ADSWAT>2.3.CO;2.

Luciani, V., 2002, High resolution planktonic foraminiferal analysis from the Cretaceous/Tertiary boundary at Ain Settara (Tunisia): Evidence of an extended mass extinction: Palaeogeography, Palaeoclimatology, Palaeoecology, v. 178, no. 3, p. 299–319, doi:10.1016/S0031-0182(01)00400-X.

MacLeod, K.G., Huber, B.T., and Isaza-Londono, C., 2005, North Atlantic warming during global cooling at the end of the Cretaceous: Geology, v. 33, p. 437–440, doi:10.1130/G21466.1.

MacLeod, K.G., Whitney, D.L., Huber, B.T., and Koeberl, C., 2007, Impact and extinction in remarkably complete Cretaceous-Tertiary boundary sections from Demerara Rise, tropical western North Atlantic: Geological Society of America Bulletin, v. 119, p. 101–115, doi:10.1130/B25955.1.

Magaritz, M., Benjamini, C., Keller, G., and Moshkovitz, S., 1992, Early diagenetic isotopic signal at the Cretaceous/Tertiary boundary, Israel: Palaeogeography, Palaeoclimatology, Palaeoecology, v. 91, no. 3, p. 291–304, doi:10.1016/0031-0182(92)90073-E.

Malarkodi, N., Keller, G., Fayazudeen, P.J., and Mallikarjuna, U.B., 2010, Foraminifera from the early Danian intertrappean beds in Rajahmundry Quarries, Andhra Pradesh, SE India: Journal of the Geological Society of India, v. 75, p. 851–863, doi:10.1007/s12594-010-0066-0.

McLean, D., 1978, A terminal Mesozoic "greenhouse": Lessons from the past: Science, v. 201, no. 4354, p. 401–406, doi:10.1126/science.201.4354.401.

McLean, D., 1985, Deccan Traps mantle degassing in the terminal Cretaceous marine extinctions: Cretaceous Research, v. 6, p. 235–259, doi:10.1016/0195-6671(85)90048-5.

Mehrotra, N.C., and Sargeant, W.A.S., 1987, Late Cretaceous to Early Tertiary dinoflagellate cysts from Narsapur Well-1, Godavari-Krishna Basin, south-India: Geobios, v. 20, p. 149–191, doi:10.1016/S0016-6995(87)80033-5.

Miller, K.G., Sherrell, R.M., Browning, J.V., Field, M.P., Gallagher, W., Olsson, R.K., Sugarman, P.J., Tuorto, S., and Wahyudi, H., 2010, Relationship between mass extinction and iridium across the Cretaceous-Paleogene boundary in New Jersey: Geology, v. 38, p. 867–870, doi:10.1130/G31135.1.

Misra, K.S., 2005, Distribution pattern, age and duration and mode of eruption of Deccan and associated volcanics: Gondwana Geological Magazine, v. 8, p. 53–60.

Molina, E., Alegret, L., Arenillas, I., Arz, J., Gallala, N., Hardenbol, J., von Salis, K., Steurbaut, E., Vanhenberghe, N., and Zaghbib-Turki, D., 2006, The global boundary stratotype section and point for the base of the Danian Stage (Paleocene, Paleogene, "Tertiary," Cenozoic) at El Kef, Tunisia—Original definition and revision: Episodes, v. 29, no. 4, p. 263–273.

Mussard, M., Le Hir, G., Fluteau, F., Lefebvre, B., and Godderis, Y., 2014, this volume, Modeling the carbon-sulfate interplays in climate changes related to the emplacement of continental flood basalts, *in* Keller, G., and Kerr, A.C., eds., Volcanism, Impacts, and Mass Extinctions: Causes and Effects: Geological Society of America Special Paper 505, doi:10.1130/2014.2505(17).

Nesbitt, H.W., and Young, G.M., 1982, Early Proterozoic climates and plate motions inferred from major element chemistry of lutites: Nature, v. 299, p. 715–717, doi:10.1038/299715a0.

Nesbitt, H.W., and Young, G.M., 1989, Formation and diagenesis of weathering profiles: The Journal of Geology, v. 97, p. 129–147, doi:10.1086/629290.

Norris, R.D., Huber, B.T., and Self-Trail, B.T., 1999, Synchroneity of the KT oceanic mass extinction and meteorite impact: Blake Nose, western North Atlantic: Geology, v. 27, p. 419–422, doi:10.1130/0091-7613(1999)027<0419:SOTKTO>2.3.CO;2.

Norris, R.D., Firth, J., Blusztajn, J., and Ravizza, G., 2000, Mass failure of the North Atlantic margin triggered by the Cretaceous-Paleogene bolide impact: Geology, v. 28, p. 1119–1122, doi:10.1130/0091-7613(2000)28<1119:MFOTNA>2.0.CO;2.

Olsson, R.K., Miller, K.G., Browning, J.V., Habib, D., and Sugarmann, P.J., 1997, Ejecta layer at the Cretaceous-Tertiary boundary, Bass River, New Jersey (Ocean Drilling Program Leg 174AX): Geology, v. 25, p. 759–762, doi:10.1130/0091-7613(1997)025<0759:ELATCT>2.3.CO;2.

Pande, K., Pattanayak, S.K., Subbarao, K.V., Navaneethakrishnan, P., and Venkatesan, T.R., 2004, 40Ar/39Ar age of a lava flow from the Bhimashankar Formation, Giravali Ghat, Deccan Traps: Proceedings of the Indian Academy of Sciences, v. 113, p. 755–758.

Pandey, J., 1990, Cretaceous/Tertiary boundary, iridium anomaly, and foraminifer breaks in the Um Sohryngkew River section, Meghalaya: Current Science, v. 59, p. 570–575.

Pardo, A., and Keller, G., 2008, Biotic effects of environmental catastrophes at the end of the Cretaceous: *Guembelitria* and *Heterohelix* blooms: Cretaceous Research, v. 29, no. 5/6, p. 1058–1073, doi:10.1016/j.cretres.2008.05.031.

Pardo, A., Ortiz, N., and Keller, G., 1996, Latest Maastrichtian and K/T boundary foraminiferal turnover and environmental changes at Agost, Spain, *in* MacLeod, N., and Keller, G., eds., The Cretaceous-Tertiary Mass Extinction: Biotic and Environmental Effects: New York, Norton Press, p. 157–191.

Prasad, B., and Pundeer, B.S., 2002, Palynological events and zones in Cretaceous-Tertiary boundary sediments of Krishna-Godavari and Cauvery Basins, India: Palaeontographica, abt. B, v. 262, p. 39–70.

Prasad, G.V.R., and Sahni, A., 2014, this volume, Vertebrate fauna from the Deccan volcanic province: Response to volcanic activity, *in* Keller, G., and Kerr, A.C., eds., Volcanism, Impacts, and Mass Extinctions: Causes and Effects: Geological Society of America Special Paper 505, doi:10.1130/2014.2505(09).

Premovic, P.I., Ilic, B.S., and Dordevic, M.G., 2012, Iridium anomaly in the Cretaceous-Paleogene boundary at Hojerup (Stevns Klint, Denmark) and Woodside Creek (New Zealand): The question of an enormous proportion of extraterrestrial component: Journal of the Serbian Chemical Society, v. 77, no. 2, p. 247–255, doi:10.2298/JSC110404178P.

Punekar, J., Mateo, P.M., and Keller, G., 2014, this volume, Effects of Deccan volcanism on paleoenvironment and planktic foraminifera: A global survey, *in* Keller, G., and Kerr, A.C., eds., Volcanism, Impacts, and Mass Extinctions: Causes and Effects: Geological Society of America Special Paper 505, doi:10.1130/2014.2505(04).

Quillévéré, F., Norris, R.D., Kroon, D., and Wilson, P.A., 2008, Transient ocean warming and shifts in carbon reservoirs during the early Danian: Earth and Planetary Science Letters, v. 265, p. 600–615, doi:10.1016/j.epsl.2007.10.040.

Raju, D.S.N., 2008, Stratigraphy of India: ONGC Bulletin Special Issue 43, no. 1, 44 p.

Raju, D.S.N., Jaiprakash, B.C., Kumar, A., Saxena, R.K., Dave, A., Chatterjee, T.K., and Mishra, C.M., 1994, The magnitude of hiatus and sea-level changes across K/T boundary in Cauvery and Krishna-Godavari Basins, India: Journal of the Geological Society of India, v. 44, p. 301–315.

Raju, D.S.N., Jaiprakash, B.C., Kumar, A., Saxena, R.K., Dave, A., Chatterjee, T.K., and Mishra, C.M., 1995, Age of Deccan volcanism across KTB in Krishna-Godavari Basin: New evidences: Journal of the Geological Society of India, v. 45, p. 229–233.

Raju, D.S.N., Jaiprakash, B.C., and Kumar, A., 1996, Paleoenvironmental setup and age of basin floor just prior to the spread of Deccan volcanism in the Krishna-Godavari Basin, India: Geological Society of India Memoir 37, p. 285–295.

Remane, J., Keller, G., Hardenbol, J., and Ben Haj Ali, M., 1999, Report on the International Workshop on Cretaceous-Paleogene Transitions: Episodes, v. 22, no. 1, p. 47–48.

Renne, P.R., Deino, A.L., Hilgen, F.J., Kuiper, F.G., Mark, D.F., Mitchell, W.S., III, Morgan, L.E., Mundil, R., and Smit, J., 2013, Time scales of critical events around the Cretaceous-Paleogene boundary: Science, v. 339, p. 684–687, doi:10.1126/science.1230492.

Rice, A., 1990, The role of volcanism in K/T extinctions, *in* Lockley, M.G., and Rice, A., eds., Volcanism and Fossil Biotas: Geological Society of America Special Paper 244, p. 39–56.

Robinson, N., Ravizza, G., Coccioni, R., Peucker-Ehrenbrink, B., and Norris, R., 2009, A high-resolution marine 187Os/188Os record for the late Maastrichtian: Distinguishing the chemical fingerprints of Deccan volcanism and the KP impact event: Earth and Planetary Science Letters, v. 281, p. 159–168, doi:10.1016/j.epsl.2009.02.019.

Sahni, A., 1983. Upper Cretaceous palaeobiogeography of Peninsular India and the Cretaceous-Paleocene transition: The vertebrate evidence, *in* Maheshwari, H.K., ed., Cretaceous of India: Lucknow, India, Indian Association of Palynostratigraphers, p. 128–140.

Samant, B., and Mohabey, D.M., 2014, this volume, Deccan volcanic eruptions and impact on flora: Palynological evidence, *in* Keller, G., and Kerr, A.C, eds., Volcanism, Impacts, and Mass Extinctions: Causes and Effects: Geological Society of America Special Paper 505, doi:10.1130/2014.2505(08).

Sant, D.A., Mathew, G., Khadkikar, A.S., Gogte, V., and Gundurao, T.K., 2003, Co-existent cristobalite and iridium at 65 Ma, Anjar intertrappeans, Kachchh, western India: Cretaceous Research, v. 24, p. 105–110, doi:10.1016/S0195-6671(03)00028-4.

Saxena, R.K., and Misra, C.M., 1994, Time and duration of Deccan volcanism in the Razole area, Krishna-Godavari Basin, India: Current Science, v. 66, no. 1, p. 73–76.

Saxena, R.K., and Misra, C.M., 1995, Campanian-Maastrichtian nannoplankton biostratigraphy of the Narsapur claystone Formation, Krishna-Godavari Basin, India: Journal of the Geological Society of India, v. 45, p. 323–329.

Schmitz, B., Keller, G., and Stenvall, O., 1992, Stable isotope changes across the Cretaceous-Tertiary boundary at Stevns Klint, Denmark: Arguments for long-term oceanic instability before and after bolide impact event: Palaeogeography, Palaeoclimatology, Palaeoecology, v. 96, p. 233–260, doi:10.1016/0031-0182(92)90104-D.

Schulte, P., Stinnesbeck, W., Stueben, D., Kramar, U., Berner, Z., Keller, G., and Adatte, T., 2003, Fe-rich and K-rich mafic spherules from slumped and channelized Chicxulub ejecta deposits in the northern La Sierrita area, NE Mexico: International Journal of Earth Sciences, v. 92, p. 114–142.

Schulte, P., Speijer, R., Mai, H., and Kontny, A., 2006, The Cretaceous-Paleogene (K-P) boundary at Brazos, Texas: Sequence stratigraphy, depositional events and the Chicxulub impact: Sedimentary Geology, v. 184, no. 1–2, p. 77–109, doi:10.1016/j.sedgeo.2005.09.021.

Schulte, P., Alegret, L., Arenillas, I., Arz, J.A., Barton, P.J., Bown, P.R., Bralower, T.J., Christeson, G.L., Claeys, P., Cockell, C.S., Collins, G.S., Deutsch, A., Goldin, T.J., Goto, K., Grajales-Nishimura, J.M., Grieve, R.A.F., Gulick, S.P.S., Johnson, K.R., Kiessling, W., Koeberl, C., Kring, D.A., MacLeod, K.G., Matsui, T., Melosh, J., Montanari, A., Morgan, J.V., Neal, C.R., Nichols, D.J., Norris, R.D., Pierazzo, E., Ravizza, G., Rebolledo-Vieyra, M., Reimold, W.U., Robin, E., Salge, T., Speijer, R.P., Sweet, A.R., Urrutia-Fucugauchi, J., Vajda, V., Whalen, M.T., and Willumsen, P.S., 2010, The Chicxulub asteroid impact and mass extinction at the Cretaceous-Paleogene boundary: Science, v. 327, p. 1214–1218, doi:10.1126/science.1177265.

Self, S., Widdowson, M., Thordarson, T., and Jay, A.E., 2006, Volatile fluxes during flood basalt eruptions and potential effects on the global environment: A Deccan perspective: Earth and Planetary Science Letters, v. 248, p. 518–532, doi:10.1016/j.epsl.2006.05.041.

Self, S., Jay, A.E., Widdowson, M., and Keszthelyi, L.P., 2008, Correlation of the Deccan and Rajahmundry Trap lavas: Are these the longest and largest lava flows on Earth?: Journal of Volcanology and Geothermal Research, v. 172, p. 3–19, doi:10.1016/j.jvolgeores.2006.11.012.

Sharma, R., and Khosla, A., 2009, Early Paleocene ostracoda from the Cretaceous-Tertiary Deccan intertrappean sequence at Jhilmili, Chhindwara District, Central India: Journal of the Palaeontological Society of India, v. 54, no. 2, p. 197–208.

Sheth, H.C., Pande, K., and Bhutani, R., 2001, ^{40}Ar/^{39}Ar age of a national geological monument: The Gilbert Hill basalt, Deccan Traps, Bombay: Current Science, v. 80, p. 1437–1440.

Smit, J., Montanari, A., Swinburne, N.H.M., Alvarez, W., Hildebrand, A.R., Margolis, S.V., Claeys, P., Lowrie, W., and Asaro, F., 1992, Tektite-bearing, deep-water clastic unit at the Cretaceous-Tertiary boundary in northeastern Mexico: Geology, v. 20, p. 99–103, doi:10.1130/0091-7613(1992)020<0099:TBDWCU>2.3.CO;2.

Smit, J., Roep, T.B., Alvarez, W., Montanari, A., Claeys, P., Grajales-Nishimura, J.M., and Bermudez, J., 1996, Coarse-grained clastic sandstone complex at the K-T boundary around the Gulf of Mexico: Deposition by tsunami waves induced by the Chicxulub impact, *in* Ryder, G., Fastovsky, D., and Gartner, S., eds., The Cretaceous-Tertiary Event and Other Catastrophes in Earth History: Geological Society of America Special Paper 307, p. 151–182.

Smit, J., van der Gaast, S., and Lustenhouwer, W., 2004, Is the transition to post-impact rock complete? Some remarks based on XRF scanning electron microprobe and thin section analyses of the Yaxcopoil-1 core: Meteoritics & Planetary Science, v. 39, p. 1113–1126, doi:10.1111/j.1945-5100.2004.tb01132.x.

Subbarao, K.V., and Pathak, S., 1993, Reversely magnetized flows, Rajahmundry, Andhra Pradesh: Journal of the Geological Society of India, v. 41, p. 71–72.

Tantawy, A.A., 2003, Calcareous nannofossil biostratigraphy and paleoecology of the Cretaceous-Tertiary transition in the western desert of Egypt: Marine Micropaleontology, v. 47, p. 323–356, doi:10.1016/S0377-8398(02)00135-4.

Vandamme, D., Courtillot, V., Besse, J., and Montigny, R., 1991, Paleomagnetism and age determinations of the Deccan Traps (India): Results of a Nagpur-Bombay traverse and review of earlier work: Reviews of Geophysics and Space Physics, v. 29, v. 159–190.

Venkatesan, T.R., Pande, K., and Gopalan, K., 1993, Did Deccan volcanism pre-date the Cretaceous-Tertiary transition?: Earth and Planetary Science Letters, v. 119, no. 1–2, p. 181–189, doi:10.1016/0012-821X(93)90015-2.

von Salis, K., and Saxena, R.K., 1998, Calcareous nannofossils across the K/T boundary and the age of the Deccan Trap volcanism in southern India: Journal of the Geological Society of India, v. 51, p. 183–192.

Ward, W., Keller, G., Stinnesbeck, W., and Adatte, T., 1995, Yucatan subsurface stratigraphy: Implications and constraints for the Chicxulub impact: Geology, v. 23, p. 873–876, doi:10.1130/0091-7613(1995)023<0873:YNSSIA>2.3.CO;2.

Watkins, D.K., and Self-Trail, J.M., 2005, Calcareous nannofossil evidence for the existence of the Gulf Stream during the late Maastrichtian: Paleoceanography, v. 20, PA3006, doi:10.1029/2004PA001121.

Wedepohl, K.H., 1971, Environmental influences on the chemical composition of shales and clays, *in* Ahrens, L.H., Press, F., Runcorn, S.K., and Urey, H.C., eds., Physics and Chemistry of the Earth: Oxford, UK, Pergamon, p. 305–333.

Wignall, P.B., 2001, Large igneous provinces and mass extinctions: Earth-Science Reviews, v. 53, p. 1–33, doi:10.1016/S0012-8252(00)00037-4.

Wilf, P., Johnson, K.R., and Huber, B.T., 2003, Correlated terrestrial and marine evidence for global climate changes before mass extinction at the Cretaceous-Paleogene boundary: Proceedings of the National Academy of Sciences of the United States of America, v. 100, no. 2, p. 599–604, doi:10.1073/pnas.0234701100.

Manuscript Accepted by the Society 31 January 2014

Printed in the USA